ETC HE Report 2023/4

Interim air quality maps of EEA member and cooperating countries for 2022

PM_{10}, O_3, and NO_2 spatial estimates and evaluation of $PM_{2.5}$ interim mapping

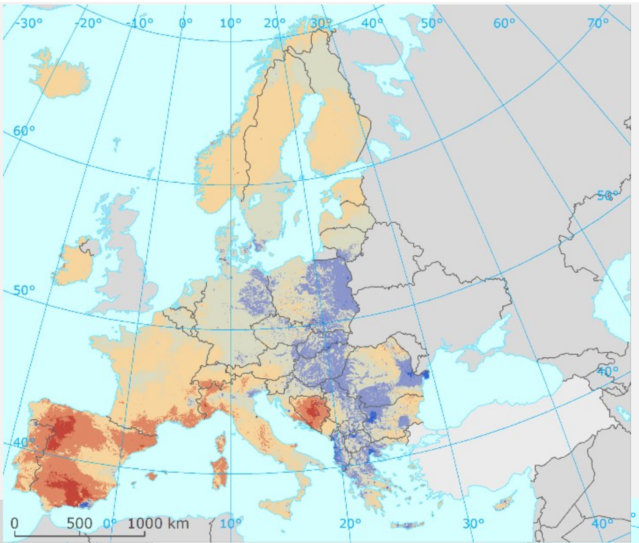

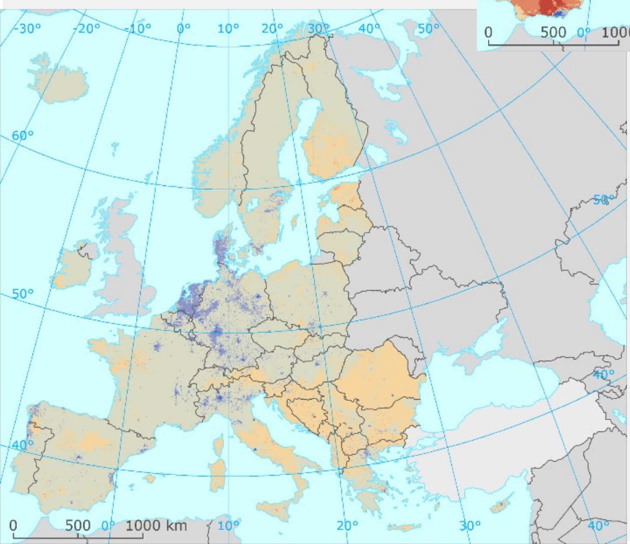

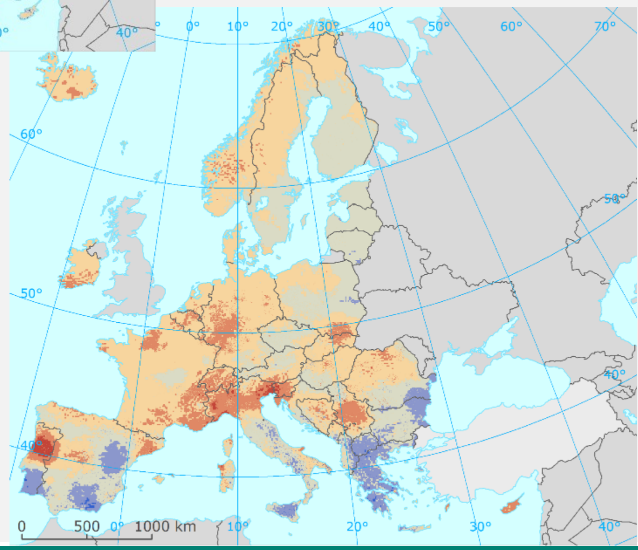

Authors:
Jan Horálek (CHMI), Leona Vlasáková (CHMI), Markéta Schreiberová (CHMI), Philipp Schneider (NILU), Nina Benešová (CHMI)

European Environment Agency
European Topic Centre
Human health and the environment

Cover design: EEA
Cover image: Maps showing differences in concentrations between five-year mean 2017-2021 and 2022 for PM_{10} annual average (top), NO_2 annual average (bottom left) and ozone indicator SOMO35 (bottom right). (This report´s Maps 4.2, 6.2 and 5.2, left.)
Back cover image: Maps showing concentrations of PM_{10} annual average (top), NO_2 annual average (bottom left) and ozone indicator SOMO35 (bottom right) for 2022. (This report´s Maps 4.1, 6.1 and 5.1.)
Layout: EEA / ETC HE (CHMI)

Publication Date: December 2023
ISBN 978-82-93970-22-4

How to cite this report:
Horálek, J., Vlasáková, J., Schreiberová, M., Schneider, P. & Benešová, N. (2023). *Interim air quality maps of EEA member and cooperating countries for 2022. PM_{10}, O_3 and NO_2 spatial estimates and evaluation of $PM_{2.5}$ interim mapping* (Eionet Report – ETC HE 2023/4). European Topic Centre on Human Health and the Environment.

The report is available from https://www.eionet.europa.eu/etcs/all-etc-reports and https://zenodo.org/communities/eea-etc/?page=1&size=20.

EEA activity no. 3 Human Health and the Environment

ETC HE coordinator: Stiftelsen NILU (The climate and environmental research institute NILU)

ETC HE consortium partners: Federal Environment Agency/Umweltbundesamt (UBA), Aether Limited,
Czech Hydrometeorological Institute (CHMI), Institut National de l'Environnement Industriel et des Risques (INERIS),
Swiss Tropical and Public Health Institute (Swiss TPH), Universitat Autònoma de Barcelona (UAB),
Vlaamse Instelling voor Technologisch Onderzoek (VITO), 4sfera Innova S.L.U., klarFAKTe.U

European Topic Centre on
Human Health and the Environment (ETC HE)
https://www.eionet.europa.eu/etcs/etc-he

Contents

Acknowledgements

The ETC task manager was Jan Horálek (CHMI, Czechia). The EEA project manager was Alberto González Ortiz.

The external task ETC/HE reviewers were Joana Soares (NILU, Norway) and Alicia Gressent (INERIS, France).

There were other ETC/HE contributions. The air quality monitoring data were extracted from the AQ e-reporting database by Anna Ripoll and Jaume Targa (4sfera, Spain). The CAMS modelling data were extracted and described by Ondřej Vlček (CHMI). The data preparation was also assisted by Jana Schovánková and Pavel Kurfürst (CHMI, Czechia).

Summary

This report presents the interim air quality maps for the area of the member and cooperating countries of the European Environmental Agency (EEA) for the year 2022. These maps are based on the non-validated up-to-date measurement data and the CAMS Ensemble Forecast modelling results, together with other supplementary data.

The interim maps and further assessment present the annual average particulate matter (PM_{10}) concentration, the annual average nitrogen dioxide (NO_2) concentration and the ground-level ozone (O_3) concentration (in terms of SOMO35).

The share of population living in the considered (i.e. presented) European area exposed to annual average PM_{10} concentration above the limit value (LV) of 40 µg/m^3 is estimated to be 0.3 %; for the EU-27, no population is estimated to be exposed to LV exceedances. More than 74 % of the both considered European and EU-27 population has been exposed to annual average concentrations above the WHO Air Quality Guideline level of 15 µg/m^3. The population-weighted concentration of the PM_{10} annual average for 2022 for the both considered European countries and for EU-27 is estimated to be about 19 µg/m^3. Population-weighted concentration of the PM_{10} annual averages show quite steady decrease in the period 2005-2022, with the lowest concentration in this period being recorded in 2020.

The share of population living both in the considered European area and the EU-27 exposed to O_3 concentration values above 6 000 µg/m^3·d (in terms of SOMO35) is estimated to be slightly more than 16 %. The population-weighted concentration of the ozone indicator SOMO35 for 2021 for the population in both considered areas is estimated to be about 4 800 µg/m^3·d. No trend is observed for the SOMO35, since ozone levels in individual years depend mainly on the meteorological conditions of the given year.

The share of population living in both the considered European and the EU-27 area exposed to annual average NO_2 concentration above the limit value (LV) of 40 µg/m^3 is estimated to be 0.2 %. Almost 72 % of the population living in both the considered European area and the EU-27 has been exposed to concentrations above the WHO Air Quality Guideline level of 10 µg/m^3. The population-weighted concentration of the NO_2 annual average for 2022 for both areas is estimated to be about 14 µg/m^3. Population-weighted concentration for the NO_2 annual average shows a steady decrease in the period 2005-2022, with the lowest concentration in this period recorded in 2020.

In addition to the production of the regular interim maps for 2022, the interim mapping for $PM_{2.5}$ has been tested for the first time. Earlier, low number of stations with the E2a data for $PM_{2.5}$ prevented the interim mapping of this pollutant (Horálek et al., 2021a). The $PM_{2.5}$ interim map for 2021 has been verified based on the validated E1a measurement data. Based on the analysis performed, the conclusion is that the uncertainty of this map is low enough to enable the interim map construction.

Based on the methodology evaluated for 2021, the $PM_{2.5}$ interim map for 2022 has been constructed. It is estimated that 0.7 % of population living in the considered (i.e. presented) European area has been exposed to concentrations above the EU annual limit value (LV) of 25 µg/m^3%; for the EU-27, almost no population (< 0.05%) is estimated to be exposed to LV exceedances. About 97 % of the population living in both the considered European area and the EU-27 has been exposed to concentrations above the WHO Air Quality Guideline level of 5 µg/m^3. The population-weighted concentration of the $PM_{2.5}$ annual average for 2022 is estimated to be 11.5 µg/m^3 for the EEA member and cooperating countries and 11.3 µg/m^3 for the EU-27.

1 Introduction

European wide air quality (AQ) annual maps have been routinely constructed under the ETC HE (and the previous consortia) since 2005 (Horálek, 2023b and references therein). The mapping methodology combines monitoring data, chemical transport model (CTM) results and other supplementary data using a linear regression model followed by kriging of the residuals produced from that model ('residual kriging'). Separate mapping layers (rural, urban background and urban traffic, where relevant) are created separately and subsequently merged together into the final map. In order to reflect the three steps applied, the methodology is called *Regression – Interpolation – Merging Mapping (RIMM)*. The regular maps (i.e. maps presented under the ETC's regular mapping reports, e.g. Horálek et al., 2023b) are based on the validated air quality monitoring data as stored in the EEA's AQ e-reporting database (in the so-called E1a data set), the modelling results and other supplementary data. Due to the time schedule of the production and availability of the validated AQ measurement data, the regular RIMM maps of a year Y are typically available in May of year Y+2. Thus, the regular 2022 maps based on the validated data will be available ca. in May 2024.

This report presents the interim air quality maps for 2022 for the area of the EEA member and cooperating countries([1]) (and the three microstates of Andorra, Monaco and San Marino). These maps are based on the non-validated up-to-date (UTD) measurement data (as available in the E2a data set of the AQ e-reporting database) and the CAMS Ensemble Forecast modelling results, together with other supplementary data. The reason for production of these interim maps is their earlier availability. The interim maps creation was previously developed and evaluated, and consequently the interim maps of PM_{10}, NO_2 and ozone were recommended for regular production, see Horálek et al. (2021a, 2021b). In order to overcome an obstacle of data gaps of the E2a data in some areas, the use of so-called pseudo stations data in the areas with the lack of E2a stations are used, based on the regression relation between the E2a data from a year Y and the validated E1a data from a year Y-1, together with the ratio of the modelling results from years Y and Y-1. The use of the pseudo station data in the interim mapping is applied for PM_{10} and NO_2. For ozone, the data coverage of the E2a data is larger and the interim ozone maps might be constructed without the use of the pseudo stations. The interim maps are not produced for the area of Türkiye, due to the lack of the E2a monitoring data from Turkish stations.

In this report, interim 2022 maps for the PM_{10} annual average, the NO_2 annual average and the ozone indicator SOMO35 are presented. Also, the difference between the five-year mean 2017-2021 and 2022 and the inter-annual difference between 2021 and 2022 are discussed. In addition, population exposure estimated based on the concentration maps is briefly shown. However, in Horálek et al. (2021b) only the spatial maps have been examined, not the exposure estimates. Thus, in this report, we provide basic exposure estimates only, not the detailed information for individual countries. The exposure estimates are presented for five large European regions (Northern Europe, Western Europe, Central Europe, Southern Europe and South-Eastern Europe), for the EU-27 and for the whole mapping area. Apart from this, the evolution of the overall population-weighted concentration in the 18-year period 2005-2022 is also shown.

In addition to the production of the regular interim maps for 2022, the interim mapping of $PM_{2.5}$ has been tested. The $PM_{2.5}$ interim map for 2021 have been verified based on the validated 2021 E1a data. Based on the methodology evaluated for 2021, the $PM_{2.5}$ interim map for 2022 has been also constructed.

([1]) The EEA member countries are 27 countries of the European Union (EU-27), Iceland, Lichtenstein, Norway, Switzerland, and Türkiye. The EEA cooperating countries are Albania, Bosnia and Herzegovina, Montenegro, North Macedonia, Serbia, and Kosovo under the UN Security Council Resolution 1244/99. In this report, Kosovo is considered individually, without prejudice on its status.

Chapter 2 describes briefly the methodological aspects and Chapter 3 presents the input data applied. Chapters 4, 5, and 6 present the concentration maps and basic exposure estimates for PM_{10}, ozone and NO_2, respectively. Chapter 7 presents the evaluation of $PM_{2.5}$ interim mapping. Chapter 8 brings the conclusions. Annex provides the technical details of the maps and their uncertainty estimates.

2 Methodology

2.1 Spatial mapping methodology

The mapping methodology used in the Regression – Interpolation – Merging Mapping method (RIMM) as routinely used in the spatial mapping under the ETC HE and its predecessors (Horálek et. al., 2023b) consists of a linear regression model followed by kriging of the residuals from that regression model (residual kriging):

$$\hat{Z}(s_0) = c + a_1 X_1(s_0) + a_2 X_2(s_0) + \cdots + a_n X_n(s_0) + \hat{\eta}(s_0) \qquad (2.1)$$

where $\hat{Z}(s_0)$ is the estimated concentration at a point s_o,

$\hat{Z}(s_0) X_1(s_0)$ is the chemical transport model (CTM) data at point s_o,

$X_2(s_0),\ldots, X_n(s_0)$ are n-1 other supplementary variables at point s_o,

$c, a_1, a_2,,\ldots, a_n$ are the n+1 parameters of the linear regression model calculated based on the data at the points of measurement,

$\hat{\eta}(s_0)$ is the spatial interpolation of the residuals of the linear regression model at point s_o, based on the residuals at the points of measurement.

For different pollutants and area types (rural, urban background, and for PM_{10}, $PM_{2.5}$ and NO_2 also urban traffic), different supplementary data are used, see Annex 1. The spatial interpolation of the regression residuals is carried out using ordinary kriging, according to

$$\hat{\eta}(s_0) = \sum_{i=1}^{N} \lambda_i \eta(s_i) \qquad \text{with } \sum_{i=1}^{N} \lambda_i = 1, \qquad (2.2)$$

where $\hat{\eta}(s_0)$ is the interpolated value at a point s_o,

N is the number of the measurement points used in the interpolation, which is fixed based on the variogram; in any case, $20 \le N \le 50$,

$\eta(s_i)$ is the residual of the linear regression model at the measurement point s_i,

$\lambda_1,\ldots, \lambda_N$ are the estimated weights based on the variogram, see Cressie (1993).

For PM_{10} and $PM_{2.5}$, prior to linear regression and interpolation, a logarithmic transformation to measurements and CTM modelled concentrations is executed. After interpolation, a back-transformation is applied.

Separate map layers are created for rural and urban background areas on a grid at resolution of 1 km (for PM_{10} and NO_2) and 10 km (for ozone), and for urban traffic areas at 1 km (for PM_{10}, $PM_{2.5}$ and NO_2). The rural background map layer is based on rural background stations, the urban background map layer on urban and suburban background stations and the potential urban traffic map layer is based on urban and suburban traffic stations. Subsequently, the separate map layers are merged into one combined final map at 1 km resolution using weight at 1 km resolution, according to

$$\hat{Z}_F(s_0) = \left(1 - w_U(s_0)\right) \cdot \hat{Z}_R(s_0) + w_U(s_0)\left(1 - w_T(s_0)\right) \cdot \hat{Z}_{UB}(s_0) + w_T(s_0) \cdot \hat{Z}_{UT}(s_0)$$

for PM_{10} and NO_2

$$= \left(1 - w_U(s_0)\right) \cdot \hat{Z}_R(s_0) + w_U(s_0) \cdot \hat{Z}_{UB}(s_0) \text{ for ozone} \qquad (2.3)$$

where $\hat{Z}_F(s_0)$ is the resulting estimated concentration in a grid cell s_o for the final map,

$\hat{Z}_R(s_0)$, $\hat{Z}_{UB}(s_0)$ and $\hat{Z}_{UT}(s_0)$ are the estimated concentrations in a grid cell s_o for the rural background, urban background and urban traffic map layers, respectively,

$w_U(s_0)$ is the weight representing the ratio of the urban character of the grid cell s_o,

$w_T(s_0)$ is the weight representing the ratio of areas exposed to traffics in a grid cell s_o.

The weight $w_U(s_0)$ is based on the population density, while the weight $w_T(s_0)$ is based on the buffers around the roads. For details of the methodology, see Horálek et al. (2023b and references therein).

In all calculations and map presentations, the EEA standard projection ETRS89-LAEA5210 is used. The mapping area covers the whole Europe apart from Belarus, Moldova, Ukraine and the European parts of Russia, Türkiye and Kazakhstan. The results for the United Kingdom are not presented, although they have been calculated. The only exception is the population-weighted concentration for showing its evolution in the 18-year period 2005-2022. In this case, the whole area including the United Kingdom is used for the calculation of this indicator.

2.2 Pseudo station data estimation

In order to supplement the E2a measurement data, which are affected by some spatial gaps, in the mapping procedure of PM and NO_2 maps we also use data from so-called *pseudo stations.* These data are concentration estimates at the locations of stations with no E2a data for the actual year Y, but with the validated E1a data for the year Y-1. As tested in Horálek et al. (2021b), these estimates are based on the relation between E2a data from year Y and validated E1a data from year Y-1, and also the ratio of the modelling or satellite data in years Y and Y-1 is used. The estimates are calculated based on the equation

$$\hat{Z}_Y(s) = c + a_1 . Z_{Y-1}(s) + a_2 . \frac{M_Y}{M_{Y-1}} . Z_{Y-1}(s) \qquad (2.4)$$

where $\hat{Z}_Y(s)$ is the estimated concentration value at a station *s* for the year *Y*,

$Z_{Y-1}(s)$ is the measurement value at a station *s* for the year *Y-1,* based on the E1a data,

$M_Y(s)$, $M_{Y-1}(s)$ are the modelling or the satellite data at a station *s* for the years *Y* and *Y-1*,

c, a_1,, a_2 are the parameters of the linear regression model calculated based on the data at the points of all stations with measurements for both *Y* and *Y-1* years.

In the case of $PM_{2.5}$, next to the above mentioned pseudo stations, other pseudo $PM_{2.5}$ stations are also used in the locations of PM_{10} stations with no $PM_{2.5}$ measurement, similarly as in the regular mapping (Horálek et al., 2023b). These estimates are based on PM_{10} measurement E2a data for the actual year Y and different supplementary data, using linear regression:

$$\hat{Z}_{PM_{2.5}}(s) = c + b . Z_{PM_{10}}(s) + a_1 X_1(s) + a_2 X_2(s) + \cdots + a_n X_n(s) \qquad (2.5)$$

where $\hat{Z}_{PM_{2.5}}(s)$ is the estimated value of $PM_{2.5}$ at the station *s*,

$Z_{PM_{10}}(s)$ is the measurement E2a value of PM_{10} at the station *s*,

c, b, a_1,,…, a_n are the parameters of the linear regression model calculated based on the data at the points of stations with both $PM_{2.5}$ and PM_{10} E2a data,

$X_1(s)$,…, $X_n(s)$ are the values of other supplementary variables at the station *s*,

n is the number of other supplementary variables used in the linear regression.

In both types of the pseudo stations estimates (i.e. based on both Eq. 2.4 and 2.5), all background stations (either classified as rural, urban or suburban) are handled together for estimating values at background pseudo stations, while all traffic stations used are applied for estimating values at traffic pseudo stations.

2.3 Uncertainty analysis

The uncertainty estimation of the interim maps is based on *leave-one-out cross-validation* using the E2a data for the mapped year. This cross-validation computes the spatial interpolation for each point of measurement from all available information except from the point in question (i.e. it withholds data of one point and then makes a prediction at the spatial location of that point). This procedure is repeated for all points of measurement in the available set. The predicted and measurement E2a values at these points are compared using statistical indicators and scatter plots. The main indicators used are root mean square error (RMSE), relative root mean square error (RRMSE) and bias (mean prediction error, MPE):

$$RMSE = \sqrt{\frac{1}{N}\sum_{i=1}^{N}\left(\hat{Z}(s_i) - Z(s_i)\right)^2} \tag{2.6}$$

$$RRMSE = \frac{RMSE}{\bar{Z}}.100 \tag{2.7}$$

$$bias(MPE) = \frac{1}{N}\sum_{i=1}^{N}\left(\hat{Z}(s_i) - Z(s_i)\right) \tag{2.8}$$

where $Z(s_i)$ is the air quality measured indicator value at the i^{th} point, $i = 1, ..., N$,

$\hat{Z}(s_i)$ is the air quality estimated indicator value at the i^{th} point using other information, without the indicator value derived from the measured value at the i^{th} point,

$\bar{Z}$ is the mean of the values $Z(s_1), ..., Z(s_N)$, as measured at points $i = 1, ..., N$,

N is the number of the measuring points.

Other indicators are R^2 and the regression equation parameters *slope* and *intercept*, following from the scatter plot between the predicted (using cross-validation) and the observed concentrations.

RMSE and RRMSE should be as small as possible, bias (MPE) should be as close to zero as possible, R^2 should be as close to one as possible, slope *a* should be as close to one as possible, and intercept *c* should be as close to zero as possible (in the regression equation $y = a.x + c$).

It should be mentioned that the uncertainty estimates are valid only for areas covered by the E2a measurements. The complete validation of the interim maps including the areas not covered by the E2a data might be done when the validated E1a data are available.

2.4 Validation

Where available, we perform the validation of both the pseudo station estimates and the concentration maps based on the validated E1a data. In this report, we perform the validation of the $PM_{2.5}$ interim mapping for 2021 (see Section 7.1). For 2022 maps, the validated E1a data are not available yet in the time designated for this report.

The validation of the pseudo station estimates is done based on the E1a measurement $PM_{2.5}$ data, where available. The statistical indicators for the validation are *standard error* and R^2.

The validation of the concentration maps is also done based on the E1a measurement $PM_{2.5}$ data. For stations with E1a $PM_{2.5}$ data and no E2a $PM_{2.5}$ data, the simple *point observation – grid prediction validation* is performed, which compares the measurement data at stations and gridded prediction values of the relevant RIMM map.

For stations with both E2a and E1a data available, the evaluation is done primarily using the *leave-one-out cross-validation*: it computes the spatial interpolation for each measurement point from all available information except from the point in question. This procedure is repeated for all measurement points in the available set. The predicted and measurement E1a values at these points are compared using statistical indicators and a scatter plot. Additionally, the simple point observation – grid prediction validation is performed also for these stations.

The results of both cross-validation and simple validation are described by the statistical indicators and scatter plots. The main indicators used are RMSE, RRMSE and bias (see Eq. 2.6-2.8). Other indicators are R^2 and the regression equation parameters, following from the scatter plot between the predicted (using either cross-validation or simple validation) and the observed concentrations.

2.5 Population exposure calculation and estimation of trends

Population exposure and population-weighted concentration for large regions, for EU-27 and for the whole presented area are calculated based on the air quality maps (and map layers) and population density data, as described in Horálek et al. (2023b). For detecting and estimating the trends in time series of annual values of population exposure, the non-parametric Mann-Kendall's test for detecting the presence of the monotonic trend and the non-parametric Sen's method for estimating the slope of a linear trend are executed, see Gilbert (1987).

2.6 Geographical division of Europe used for the assessment

The tables of population exposure and population-weighted concentration present the country grouping of the following large regions: 1) Northern Europe (N): Denmark (including Faroes), Estonia, Finland, Iceland, Latvia, Lithuania, Norway, Sweden; 2) Western Europe (without UK) (W): Belgium, France north of 45°, Ireland, Luxembourg, Netherlands; 3) Central Europe (C): Austria, Czechia, Germany, Hungary, Liechtenstein, Poland, Slovakia, Slovenia, Switzerland; 4) Southern Europe (S): Andorra, Cyprus, France south of 45°, Greece, Italy, Malta, Monaco, Portugal, San Marino, Spain; 5) South-eastern Europe (SE): Albania, Bosnia and Herzegovina, Bulgaria, Croatia, Montenegro, North Macedonia, Romania, Serbia, and Kosovo.

3 Data used

3.1 Air quality monitoring data

For the interim maps, we have used air quality station 2021 (for $PM_{2.5}$ only) and 2022 monitoring data coming from the E2a data set of the Air Quality e-Reporting database (EEA, 2022, 2023a). The data of the up-to-date (UTD) dataflow E2a are being provided on an hourly basis from most of the EEA's member and cooperating countries. This data set has been supplemented with British stations(2) from the Defra database (Defra, 2023).

For the purposes of the pseudo stations calculations and validation (for $PM_{2.5}$ only), the 2020 and 2021 data of the E1a data set of the Air Quality e-Reporting database (EEA, 2023a) have been used. The data of the dataflow E1a is submitted to EEA by the reporting countries every September and covers the year before the delivery. This E1a data set has been supplemented with several EMEP rural stations from the database EBAS (NILU, 2023) not reported to the Air Quality e-Reporting database and for 2021 also with British stations from the Defra database (Defra, 2023).

The following pollutants and aggregations are considered:

PM_{10} – annual average [µg/m^3], years 2021 (E1a and E2a) and 2022 (E2a),
$PM_{2.5}$ – annual average [µg/m^3], years 2020 (E1a), 2021 (E1a and E2a) and 2022 (E2a),
Ozone – SOMO35 [µg/m^3·d], year 2022,
NO_2 – annual average [µg/m^3], years 2021 (E1a) and 2022 (E2a).

For PM_{10}, $PM_{2,5}$ and NO_2 we use the stations classified as background (for all the three types of area, i.e. rural, suburban and urban), and also traffic for the types of area suburban and urban. For ozone, we use only data from stations classified as background (for the three types of area). In the mapping, rural background stations are used for the rural map layer, urban and suburban stations for the urban background map layer and urban and suburban traffic stations for the urban traffic map layer (Section 2.1). Industrial stations are not used, as their local concentration levels cannot be easily generalized for the whole map. Only stations with annual data coverage of at least 75 percent are used.

Table 3.1 shows the number of the stations used in the 2022 interim mapping of PM_{10} and NO_2. In the RIMM mapping (as described in Section 2.1) of the year 2022, E2a 2022 stations are used, together with pseudo stations derived from E1a stations of the year 2021. The pseudo stations are located at the places of the E1a 2021 stations with no (or not sufficient) E2a data for year 2022 (labelled "For pseudo 2022"). The rest of the E1a 2021 stations (with both E1a data for 2021 and E2a data for 2022, labelled "For regression") are used for estimation of the parameters of the linear regression for the pseudo stations calculation (see Eq. 2.4).

Table 3.1: Number of stations used in interim mapping 2022 per station type, for PM_{10} (left) and NO_2 (right)

Station type	PM_{10}				NO_2			
	E1a 2021			E2a 2022	E1a 2021			E2a 2022
	Total	For regression	For pseudo 2022	Mapping 2022	Total	For regression	For pseudo 2022	Mapping 2022
Rural background	400	301	99	311	475	406	69	417
Urban/suburb. backgr.	1445	1061	384	1114	1382	1167	215	1215
Urban/suburb. traffic	783	613	170	654	1215	757	458	803

(2) The United Kingdom exited the European Union in January 2020 and does not report the air quality data to the AQ e-reporting database. Nevertheless, in order to enable the interpolation across the whole mapping domain, the publicly available British data from the Defra database have been also used in the analysis.

Table 3.2 shows the number of the stations used in the interim mapping of ozone. In the ozone interim mapping, E2a 2022 stations are used. No pseudo stations for ozone are used, due to quite complete spatial coverage of the E2a ozone data.

Table 3.2: Number of stations used in interim mapping 2022 per station type, for ozone

Station type	Ozone
	E2a 2022
	Mapping 2022
Rural background	481
Urban/suburb. backgr.	1018

Table 3.3 shows the number of the stations used in both mapping and validation of the 2021 interim mapping of $PM_{2.5}$. Validation has been performed based on the E1a stations.

Table 3.3: Number of stations used in $PM_{2.5}$ interim mapping 2021 and its validation per station type

Station type	PM_{10}			$PM_{2.5}$				
	E2a 2021			E1a 2020			E2a 2021	E1a 2021
	Total	For regression	For pseudo $PM_{2.5}$	Total	For regression	For pseudo 2021	Mapping 2021	Validation 2022
Rural background	251	134	117	228	145	83	154	244
Urban/suburb. backgr.	987	548	439	724	520	224	596	883
Urban/suburb. traffic	573	303	270	384	293	81	331	430

Map A.1 of Annex shows the spatial distribution of the rural, urban/suburban background and urban/suburban traffic stations used in the interim 2021 $PM_{2.5}$ mapping (in green and orange) and validation (in red). In all figures, the true stations (in green) and the pseudo stations (in orange) are distinguished.

Table 3.4 shows the number of stations used in the 2022 interim mapping of $PM_{2.5}$, similar to what table 3.1 shows for PM_{10} and NO_2.

Table 3.4: Number of stations used in $PM_{2.5}$ interim mapping 2022 for each station type

Station type	PM_{10}			$PM_{2.5}$			
	E2a 2022			E1a 2021			E2a 2022
	Total	For regression	For pseudo $PM_{2.5}$	Total	For regression	For pseudo 2022	Mapping 2022
Rural background	291	164	127	245	171	74	184
Urban/suburb. backgr.	1 036	641	395	915	642	273	710
Urban/suburb. traffic	627	349	278	441	348	93	383

3.2 Chemical transport modelling (CTM) data

The CAMS Ensemble Forecast data as provided by the Copernicus Atmosphere Monitoring Service (CAMS) at a regional scale over Europe have been used. The European regional production consists of an ensemble of eleven air quality models run operationally (MINNI and MONARCH models have been added to existing ones in June 2022). All models use the same CAMS-REG anthropogenic emissions and current meteorology from the operational ECMWF IFS forecast. The models provide (along with other products) a 96-hour forecast made available at 08:00 UTC the day of the forecast. The forecast data product is available on an hourly time resolution and at a spatial resolution of 0.1° x 0.1°, which corresponds roughly to 5-10 km x 10 km. Each model forecast is combined into an ensemble forecast by taking the median of all used models. For further details see ECMWF (2023).

In this study, the CAMS Ensemble Forecast data (for the lead hour 0-23) for 2020, 2021 and 2022 have been used (METEO FRANCE et al., 2022). All the models used in the ensemble were run using the CAMS-REG-v5.1 REF2 v2.0.1 emissions representative of 2018 for most of the year 2022 (implemented in March), while before March 2022 CAMS-REG-AP_v4.2_REF2.1 representative of 2017 were used ECMWF (2023). For more information on emissions, see Kuenen et al., 2021. All modelling data have been aggregated into the annual statistics and converted into the reference EEA 1 km (for PM and NO_2) and 10 km (for O_3) grids. The pollutants and parameters used are the same as for the monitoring data.

3.3 Satellite data

Data from the TROPOspheric Monitoring Instrument (TROPOMI) onboard of the Sentinel-5 Precursor satellite (Veefkind et al., 2012) was used. Their spatial resolution is approximately 5.5 km by 3.5 km. The product used is the S5P_OFFL_L2__NO2 product (van Geffen et al., 2020) and it provides the tropospheric vertical column density of nitrogen dioxide (NO_2), i.e. a vertically integrated value over the entire troposphere. All overpasses for a specific day were then mosaicked and gridded into the reference EEA 1 km grid in the ETRS89 / ETRS-LAEA (EPSG 3035) projection. The daily gridded files have been subsequently averaged to an annual mean. The annual mean has been aggregated from cloud-free high-quality (qa_value > 0.75) daily data only. The parameter used is

NO_2 – annual average tropospheric vertical column density (VCD) [number of NO_2 molecules per cm^2 of earth surface], years 2021 and 2022.

3.4 Other supplementary data

Meteorological data

The meteorological data used are the ECWMF data extracted from the CDS (Climate Data Store, https://cds.climate.copernicus.eu/cdsapp#!/home). Specifically, the hourly data of the reanalysed data set ERA5-Land in 0.1°x0.1° resolution have been used. In the coastal areas (where the data from ERA5-Land are not available), the same parameters from the reanalysed data set ERA5 in 0.25°x0.25° resolution have been applied. The hourly data have been derived into the parameters needed, aggregated into the annual statistics and converted into the reference EEA 1 km (for PM and NO_2) and 10 km (for ozone) grids. For details, see Horálek et al. (2023b). Meteorological parameters used are *wind speed* (annual mean for 2021 and 2022, in $m.s^{-1}$), *surface net solar radiation* (annual mean of daily sum for 2021 and 2022, in $MWs.m^{-2}$) and *relative humidity* (annual mean for 2022, in percentage).

Altitude

The altitude data field (in m) of Global Multi-resolution Terrain Elevation Data 2010 (GMTED2010) has been used, with an original grid resolution of 15 arcseconds coming from U.S. Geological Survey Earth Resources Observation and Science, see Danielson and Gesch (2011). The data were converted into the EEA reference grids in 1 km and 10 km resolutions. Next to this, another aggregation based on the 1 km grid cells has been executed, i.e. the average of the circle with a radius of 5 km, calculated as a floating average for all 1 km grid cells.

Land cover

CORINE Land Cover 2018 – grid 100 m, Version 2020_20 (EU, 2020) is used. The 44 CLC classes have been re-grouped into the 8 more general classes. In this paper, we use five of these general classes, namely high density residential areas (HDR), low density residential areas (LDR), agricultural areas (AGR), natural areas (NAT), and traffic areas (TRAF). For details, see Horálek et al. (2023b). Two aggregations are used, i.e., into 1 km grid and into the circle with radius of 5 km. The aggregated grid value represents for each general class the total area of this class as percentage of the total area of the 1 km x 1 km square or the circle with radius of 5 km.

Population density and Road data

Population density (in inhabitants/km^2, census 2011) is based on Geostat 2011 grid dataset (Eurostat, 2014). For regions not included in the Geostat 2011 dataset we use as alternative sources JRC and ORNL data. For details, see Horálek et al. (2023b).

GRIP vector road type data is used (Meijer et al., 2018). Based on these data (i.e., buffers around the roads), traffic map layers (Section 2.1) are merged into the final maps (Horálek et al., 2023b).

4 Particulate matter PM_{10}

Map 4.1 presents the interim map for the PM_{10} annual average 2022, as the result of interpolation and merging of the separate map layers as described in Section 2.1 (for technical details of this map, see Annex, Section A.1). Red and dark red areas indicate concentrations above the EU annual limit value (LV) of 40 µg/m^3. Dark green indicates the areas where the PM_{10} annual average concentration is below the WHO Air Quality Guideline level of 15 µg/m^3 (WHO, 2021).

Map 4.1: Interim concentration map of PM_{10} annual average, 2022

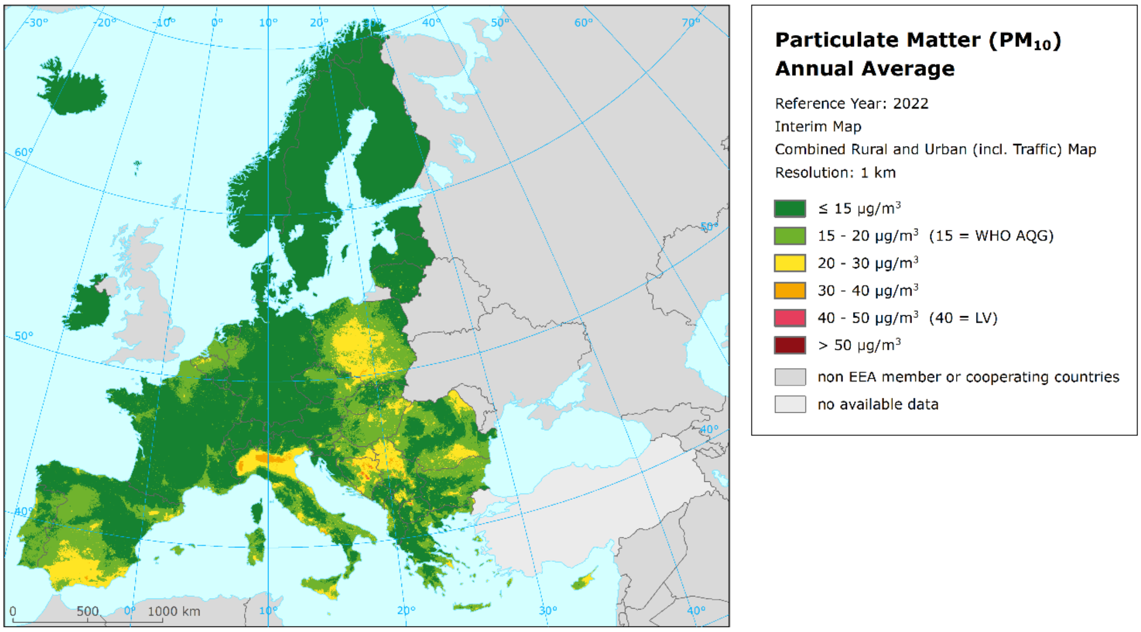

The map shows concentrations above the annual LV only in urban areas around some Balkan cities (in Bosnia and Herzegovina, Northern Macedonia and Serbia). In addition to these countries, there are areas in the Po Valley, in Italy, and smaller disconnected areas in Poland, Spain, Bosnia and Herzegovina, Serbia and Greece where PM_{10} concentrations of 30-40 µg/m^3 have been estimated. The remaining parts of Europe show concentrations below 20 µg/m^3, with concentrations below 15 µg/m^3 estimated for most of western (except parts of Benelux), central (except Poland, Hungary and parts of the Czech Republic and Slovakia) and northern Europe.

The relative mean uncertainty (Relative RMSE) of this map is 19 % for rural areas and 17 % for urban background areas (Table A.2). However, these uncertaity estimates are based on the non-validated E2a data and are valid only for areas covered by the E2a stations. The complete validation of the interim PM_{10} map can only be done when the validated E1a data for 2022 are available.

Map 4.2 shows the difference between the five-year mean 2017-2021 and 2022 and the inter-annual difference between 2021 and 2022 (using the regular maps for 2017-2021 and the 2022 interim map) for PM_{10} annual average. Orange to red areas show an increase of PM_{10} concentration in 2022, while blue areas show a decrease.

Compared to the five-year mean 2017-2021, the highest increases in annual mean PM_{10} concentrations (> 5 µg/m^3) are observed in Spain and Bosnia and Herzegovina. Increases > 2 µg/m^3 are observed in parts of southern Europe (other parts of Spain, Portugal, southern France, parts of Italy) and south-eastern Europe (the rest of Bosnia and Herzegovina). On the other hand, relatively continuous areas of central and south-eastern Europe show a decrease in annual average PM_{10}, with the deepest decreases in parts of Poland, Romania, Bulgaria, Greece and Albania. No change or slight increases/decreases of about 2 µg/m^3 are observed in most of Europe (France, parts of central, southern and south-eastern Europe and almost all of northern Europe).

Based on the map of the inter-annual difference between 2021 and 2022, there is no change or only slight increases or decreases in annual average PM_{10} concentrations in almost the entire considered (i.e. presented) European area. Nevertheless, increases in concentrations are particularly evident in Spain and Portugal, parts of France and in Bosnia and Herzegovina. Decreases in concentrations have been observed mainly in Poland and parts of some states in south-eastern Europe (North Macedonia, Albania, Greece, Bulgaria and Romania).

Map 4.2: Difference in concentrations between five-year mean 2017-2021 (left) or 2021 (right) and 2022 (based on the interim map) for PM_{10} annual average

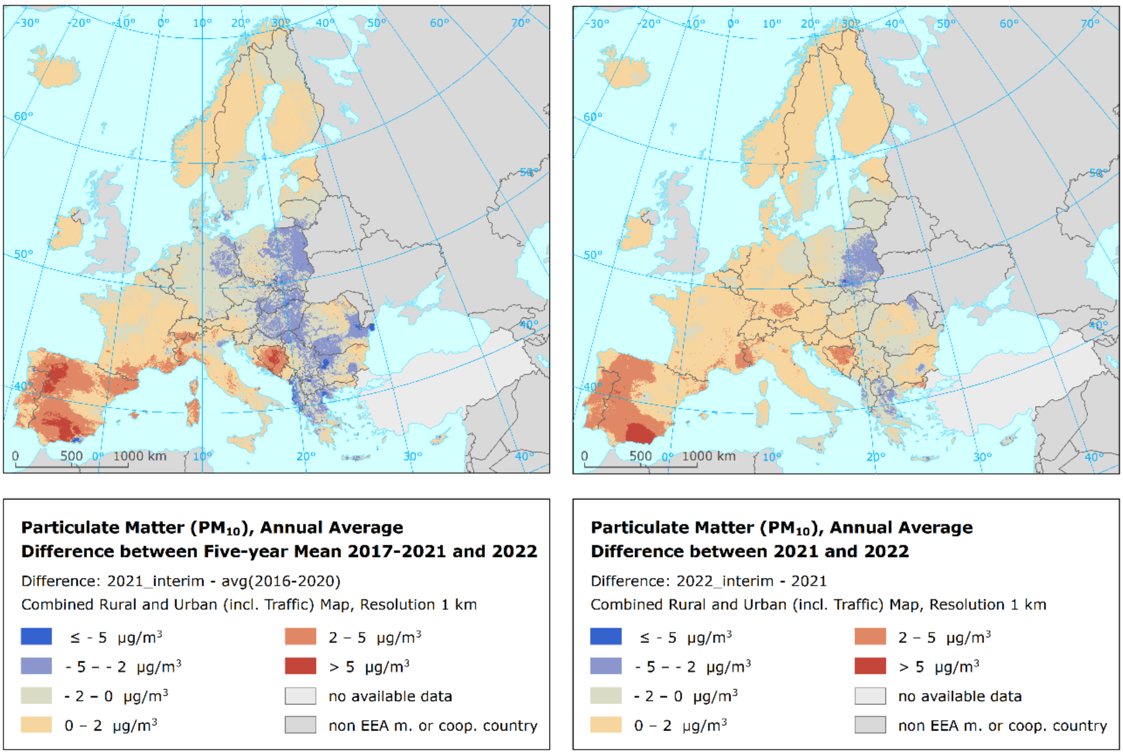

Based on the mapping results and the population density data, the population exposure estimates have been calculated. Table 4.1 gives the population frequency distribution for a limited number of exposure classes and the population-weighted concentration for five large European regions, for EU-27 and for the total presented area. The exposure estimates for individual countries is not presented, due to their high uncertainty. As presented in Horálek et al. (2023a), the exposure estimates based on interim maps give good results for the total area and the EU-27, but somewhat poorer results for individual countries.

Table 4.1: Population exposure and population-weighted concentration, PM_{10} annual average, 2022, based on the interim map

Area	Population [inhbs·1000]	PM_{10} – annual average, exposed population, 2022 [%]						PM_{10} ann. avg.
		< 15 µg/m³	15-20 µg/m³	20-30 µg/m³	30-40 µg/m³	40-50 µg/m³	> 50 µg/m³	Pop. weighted [µg/m³·inhbs⁻¹]
Northern Europe	33 656	86.9	9.6	3.5				11.5
Western Europe (without UK)	85 680	26.4	67.4	6.2				16.5
Central Europe	166 396	37.4	37.0	24.2	1.4			17.5
Southern Europe	141 374	5.7	30.9	53.5	9.8			22.2
South-eastern Europe	46 834	5.3	23.1	53.6	15.0	2.8	0.2	24.3
Total	**473 939**	**25.9**	**37.1**	**31.6**	**5.1**	**0.3**	**0.0**	**19.1**
EU-27	**442 153**	**25.2**	**38.9**	**32.0**	**3.9**			**18.8**

Note: Empty cells mean no population in exposure.

Based on the interim map, it is estimated that 0.3 % of population living in the considered (i.e. presented) European area has been exposed to concentrations above the EU annual limit value (ALV) of 40 µg/m³. All of them live in south-eastern Europe, where the share is 3 %. All of them live outside EU-27. More than 74 % of both the considered European and the EU-27 population has been exposed to annual average concentrations above the WHO Air Quality Guideline level of 15 µg/m³ (WHO, 2021). The population-weighted concentration of the PM_{10} annual average for 2022 both for the considered European countries and for EU-27 is estimated to be about 19 µg/m³.

Figure 4.1 shows, for the whole mapped area, the population frequency distribution for exposure classes with a width of 1 µg/m³. The highest population frequency is found for classes between 13 and 17 µg/m³. A quite continuous decline of population frequency is visible for classes between 20 and 30 µg/m³ and beyond 35 µg/m³.

Figure 4.1: Population frequency distribution, PM_{10} annual average 2022, based on an interim map. The WHO AQG level (15 µg/m³) is marked by the green line, the old 2005 WHO AQG level (20 µg/m³) is marked by the yellow line, the EU annual limit value (40 µg/m³) is marked by the red line

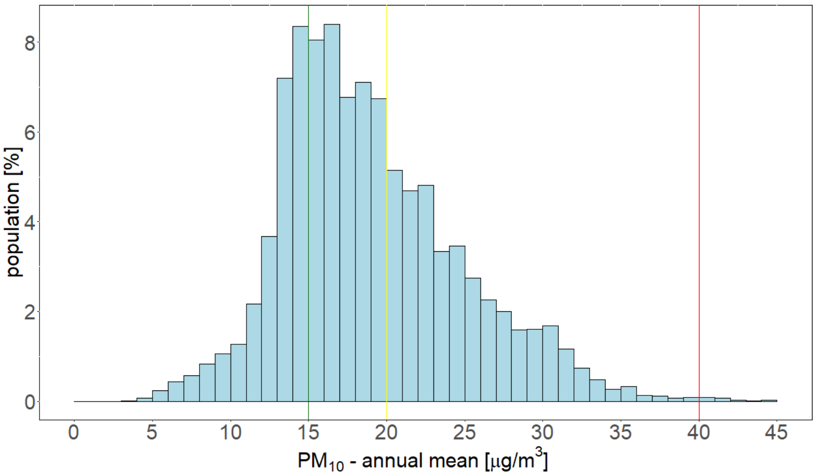

Note: Apart from the population distribution shown in graph, it was estimated that 0.1 % of population lived in areas with PM_{10} annual average concentration in between 45 and 58 µg/m³.

For changes in the population-weighted concentration of the PM_{10} annual average in the 18-year period 2005-2022, see Figure 4.2. For the previous years, mapping results as presented in Horálek et al. (2023b and references therein) have been used. Since 2017 results, PM_{10} maps were prepared based on the updated method (taking into account air quality in urban traffic areas). Furthermore, the updated method was also used to remap years 2005, 2009 and 2015-2016. For comparability reasons, results for 2005, 2009 and 2015-2019 are presented in two variants, i.e. based on both the old and the updated methodologies. Another issue is that for the 16-year time series 2005-2020, the overall population-weighted mean included the United Kingdom. Therefore, for consistency reasons, the population-weighted concentration for the whole area including the United Kingdom is presented also for 2022. This value was easily available, as the mapping domain includes the United Kingdom (see Section 2.1).

Figure 4.2: Population-weighted concentration of the PM_{10} annual average in 2005-2022, based on both the old (blue) and the updated (red) mapping methodology (where available), and with interim results for the year 2022

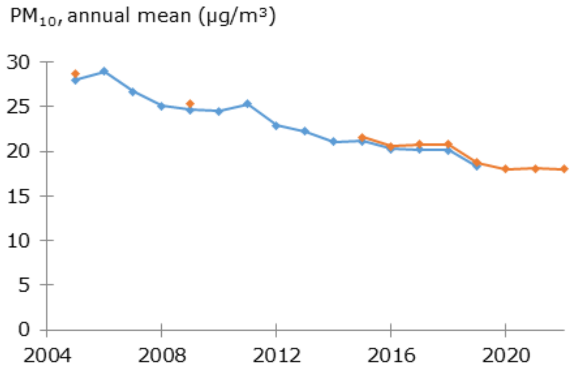

Throughout the whole period 2005-2022, the PM_{10} annual average concentrations show a quite steady decrease of about 0.6 µg/m^3 per year. One can see that the last three years 2020, 2021 and 2022 (based on the interim data) give the lowest results in the 18-year period, showing quite similar levels in these three years.

5 Ozone

Map 5.1 presents the interim 2022 map for SOMO35 as a result of merging separate rural and urban interpolated map layers as described in Section 2.1 (for technical details of this map, see Annex, Section A.2). Red and purple areas show values above 8 000 µg/m^3·d, while the orange areas show values[3] above 6 000 µg/m^3·d.

Generally, southern Europe shows higher ozone SOMO35 concentrations than northern Europe. Higher levels of ozone also occur more frequently in mountainous areas south of 50 degrees latitude than in lowlands. In 2022, SOMO35 levels > 6 000 µg/m^3·d were estimated in almost all of Italy, in much of the Balkan countries, in a large area of Spain and France, in central Europe (parts of Germany, Austria, Hungary, Switzerland) and even in small parts of northern Europe in Iceland and Norway.

Map 5.1: Interim concentration map of ozone indicator SOMO35, 2022

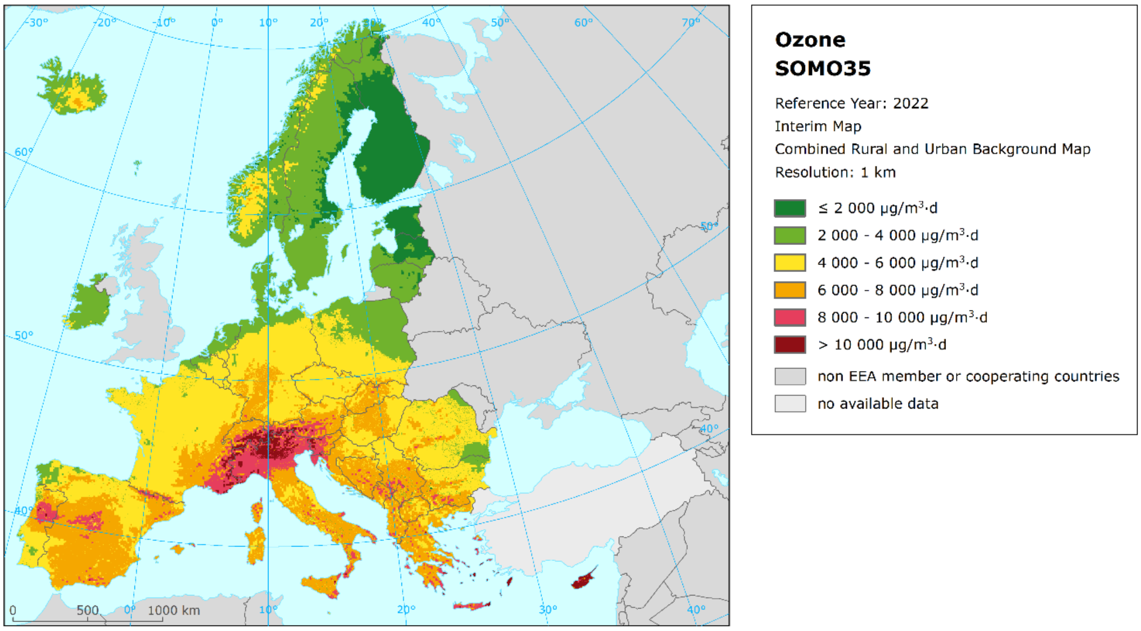

The relative mean uncertainty (Relative RMSE) of this map is 23 % for rural and 25 % for urban background areas (Table A.3). However, these uncertainty estimates are based on the non-validated E2a data and are valid only for areas covered by the E2a stations. The complete validation of the interim ozone map can only be done when the validated E1a data for 2022 are available.

Map 5.2 shows the difference between the five-year mean 2017-2021 and 2022 and the inter-annual difference between 2021 and 2022 (using the regular maps for 2017-2021 and the 2022 interim map) for the ozone indicator SOMO35. Orange to red areas show an increase of ozone concentration in 2022, while blue areas show a decrease.

Compared to the five-year mean 2017-2021, the highest increases of ozone SOMO35 concentrations (> 2 000 µg/m^3·d) in 2022 are observed in parts of Portugal and Italy. Increases > 800 µg/m^3·d are observed in parts of some other southern European states, but also in parts of central and even northern European countries. On the other hand, relatively continuous areas of southern and south-eastern Europe show a decrease in ozone SOMO35 concentrations. In most of Europe no changes or a slight increase/decrease of about 800 µg/m^3·d are observed.

[3] For a more detailed derivation of the value 6 000 µg/m^3·d see e.g. Horálek, J. et al. (2023b).

Based on the map of the inter-annual difference between 2021 and 2022, increase in ozone SOMO35 concentrations is evident in a large continuous area of central and western Europe with extends into southern Europe (France, northern Italy and Spain) and south-eastern Europe (Romania, Slovenia, Croatia, Bosnia and Herzegovina, Serbia). Within this area, the highest increases in ozone concentrations (> 2 000 μg/m^3·d) are observed in parts of France, Germany and Slovenia. Another area with an increase above 2 000 μg/m^3·d is observed in Portugal. Decreases in concentrations have been observed mainly in south-eastern Europe (North Macedonia, Albania, Greece, parts of Bulgaria and Romania). There is no change or a slight increase or decrease in ozone concentrations in almost the entire nothern Europe and southern Europe (large part of Spain, Portugal, Italy and part of the Balkan states).

Map 5.2: Difference in concentrations between five-year mean 2017-2021 (left) or 2021 (right) and 2022 (based on the interim map) for ozone indicator SOMO35

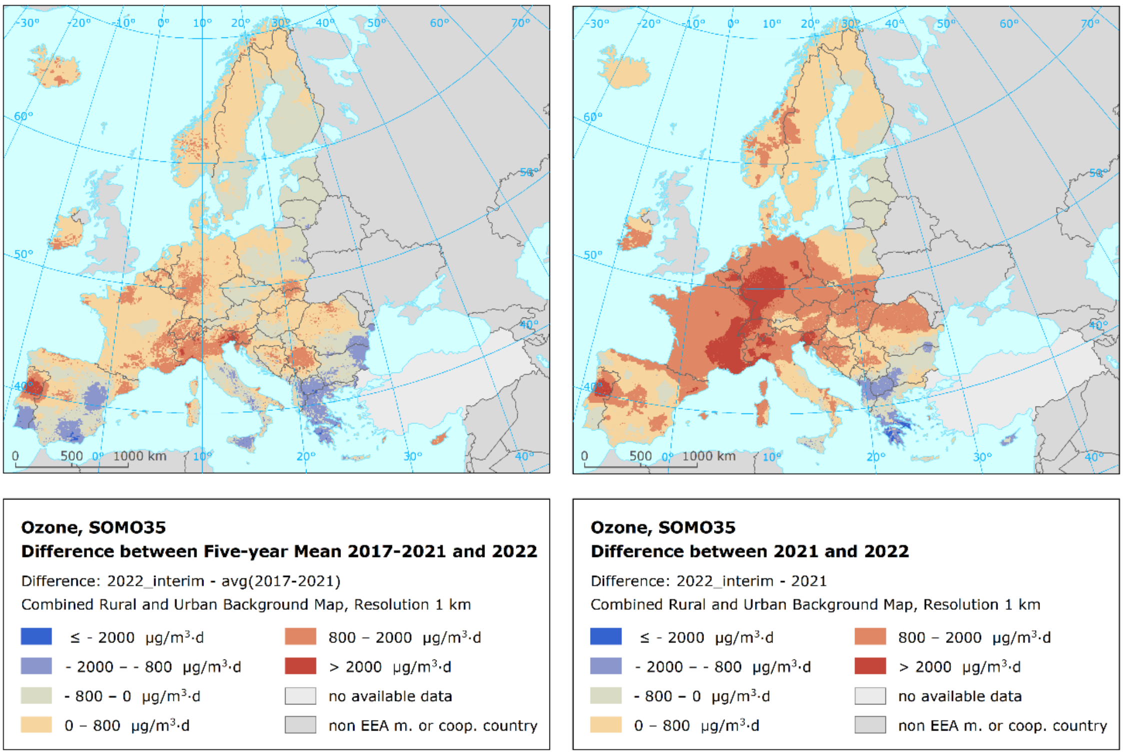

Based on the mapping results and the population density data, the population exposure estimate has been calculated. Table 5.1 gives the population frequency distribution for a limited number of exposure classes and the population-weighted concentration for large European regions, for EU-27 and for the total mapping area. The exposure estimates for individual countries is not presented, due to their high uncertainty. As presented in Horálek et al. (2023a), the exposure estimates based on interim maps give good results for the total area and the EU-27, but somewhat poorer results for individual countries.

Based on the interim map, it is estimated that more than 16 % of the both considered European and EU-27 population lived in areas with SOMO35 values above 6 000 μg/m^3·d. The population-weighted concentration of the SOMO35 for 2021 for the both considered European and EU-27 population is estimated to be about 4 800 μg/m^3·d.

Table 5.1: Population exposure and population-weighted concentration, ozone indicator SOMO35, 2022, based on an interim map

Area	Population [inhbs·1000]	Ozone – SOMO35, exposed population, 2022 [%]						Ozone – SOMO35
		< 2 000 µg/m³·d	2 000 - 4 000 µg/m³·d	4 000 - 6 000 µg/m³·d	6 000 - 10 000 µg/m³·d	8 000 - 10 000 µg/m³·d	> 10 000 µg/m³·d	Pop. weighted [µg/m³·d ·inhbs⁻¹]
Northern Europe	33 656	53.4	46.5	0.1	0.0			2 067
Western Europe (without UK)	85 680	1.3	45.7	50.4	2.6	0.1	0.0	4 098
Central Europe	166 396		19.9	69.9	9.7	0.5	0.1	4 811
Southern Europe	141 374	0.2	13.5	46.6	22.5	13.7	3.4	5 905
South-eastern Europe	46 834	7.6	40.5	44.6	7.0	0.4	0.0	4 126
Total	**473 939**	**4.8**	**26.5**	**52.0**	**11.4**	**4.3**	**1.1**	**4 755**
EU-27	**442 153**	**4.5**	**26.7**	**52.3**	**10.8**	**4.6**	**1.1**	**4 755**

Note: The percentage value "0.0" indicates that an exposed population exists, but it is small and estimated to be less than 0.05 %. Empty cells mean no population in exposure.

Figure 5.1 shows, for the whole mapped area, the frequency distribution of SOMO35 for population exposure classes of 250 µg/m³·d. The highest frequencies are found for classes between 4 000 and 5 500 µg/m³·d. One can see a decline of population frequency for exposure classes between 5 000 and 7 000 µg/m³ and a continuous mild decline of population frequency for classes above 7 000 µg/m³·d.

Figure 5.1: Population frequency distribution, ozone indicator SOMO35, 2022, based on the interim map

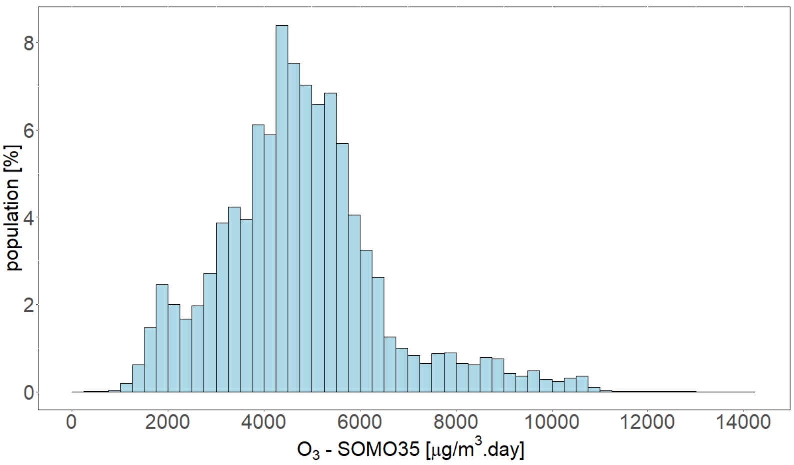

For changes in the population-weighted concentration in the period 2005-2022, see Figure 5.2. Like for PM_{10}, the population-weighted concentration for the whole area including the United Kingdom, for consistency, is presented for the whole period including the year 2022. No trend is observed for SOMO35, since ozone levels in individual years strongly depend on the meteorological conditions of the given year.

Figure 5.2: Population-weighted concentration of the ozone indicator SOMO35 in 2005-2022 (interim results for 2022)

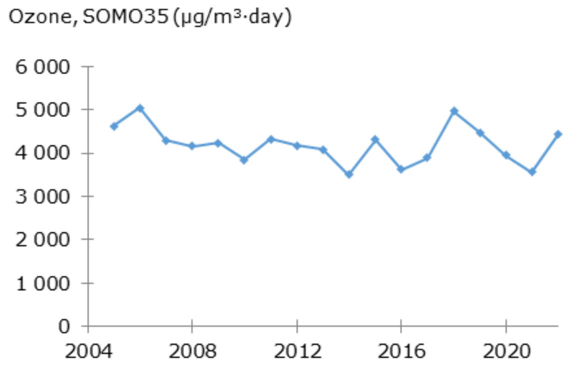

6 Nitrogen dioxide

Map 6.1 presents the interim map for the NO_2 annual average 2021, as the result of interpolation and merging of the separate map layers as described in Section 2.1 (for technical details of this map, see Annex 1, Section A.3). Red and purple areas indicate concentrations above the annual limit value (LV) of 40 µg/m^3. Dark green areas indicate concentrations below 10 µg/m^3, being the 2021 WHO Air Quality Guideline level (WHO, 2021).

The areas with highest concentrations, but in 2022 below the annual limit value of 40 µg/m^3 for NO_2, include urbanized parts of some large cities, particularly Paris, Rome, Naples, Milan, Madrid, Barcelona and Athens. Areas above 20 µg/m^3 can be found in the Po Valley, the Benelux, the German Ruhr region, in the Île de France region, around Rome and Naples and in the Krakow – Katowice (PL) – Ostrava (CZ) industrial region. Some other cities show NO_2 levels above 20 µg/m^3. Most of the European area shows NO_2 levels below 20 µg/m^3 or even below 10 µg/m^3.

Map 6.1: Interim concentration map of NO_2 annual average, 2022

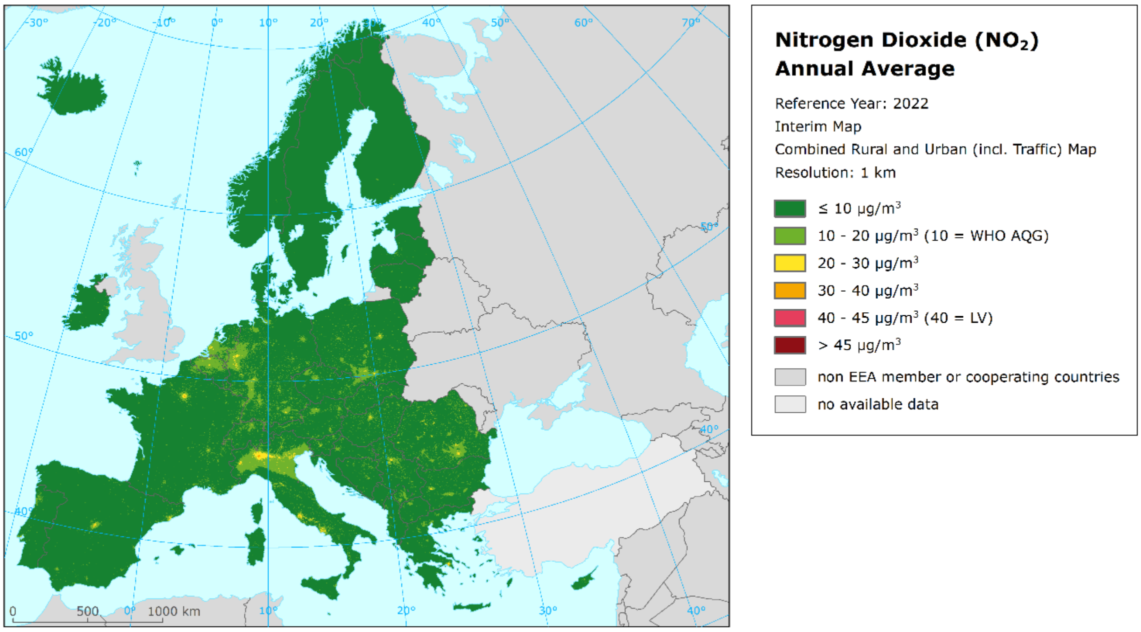

The relative mean uncertainty (Relative RMSE) of this map is 28 % for rural areas and 24 % for urban background areas (Table A.5). However, these uncertainty estimates are based on the non-validated E2a data and are valid only for areas covered by the E2a stations. The complete validation of the interim NO_2 map can only be done when the validated E1a data for 2022 are available.

Map 6.2 shows the difference between five-year mean 2017-2021 and 2022 and the inter-annual difference between 2021 and 2022 (using the regular maps for 2017-2021 and the 2022 interim map) for the NO_2 annual average. Orange to red areas show an increase of NO_2 concentration in 2022, while blue areas show a decrease.

Compared to the five-year mean 2017-2021, the highest increases in annual mean NO_2 concentrations (> 2 µg/m^3) are only seen in very small fragmented areas in Finland, Estonia, Poland and France. On the other hand, relatively continuous areas in Denmark, Netherlands and Germany show a decrease in annual average NO_2 bigger than 2 µg/m^3. No change or slight increases/decreases of about 2 µg/m^3 are observed in almost the entire considered (i.e. presented) European area.

Based on the map of the inter-annual difference between 2021 and 2022, there is no change or a slight increase/decrease in annual average NO_2 concentrations in almost the entire considered (i.e.

presented) European area. Increases in concentrations > 2 µg/m^3 are particularly evident in small parts of Spain and France. Many very small, fragmented areas with this increase can be found across all countries in considered (i.e. presented) European area. Decreases in concentrations have been observed mainly in the Po Valley in northern Italy, in Denmark, Cyprus and a small area in western Bulgaria.

Map 6.2: Difference in concentrations between five-year mean 2017-2021 (left) or 2021 (right) and 2022 (based on the interim map) for NO_2 annual average

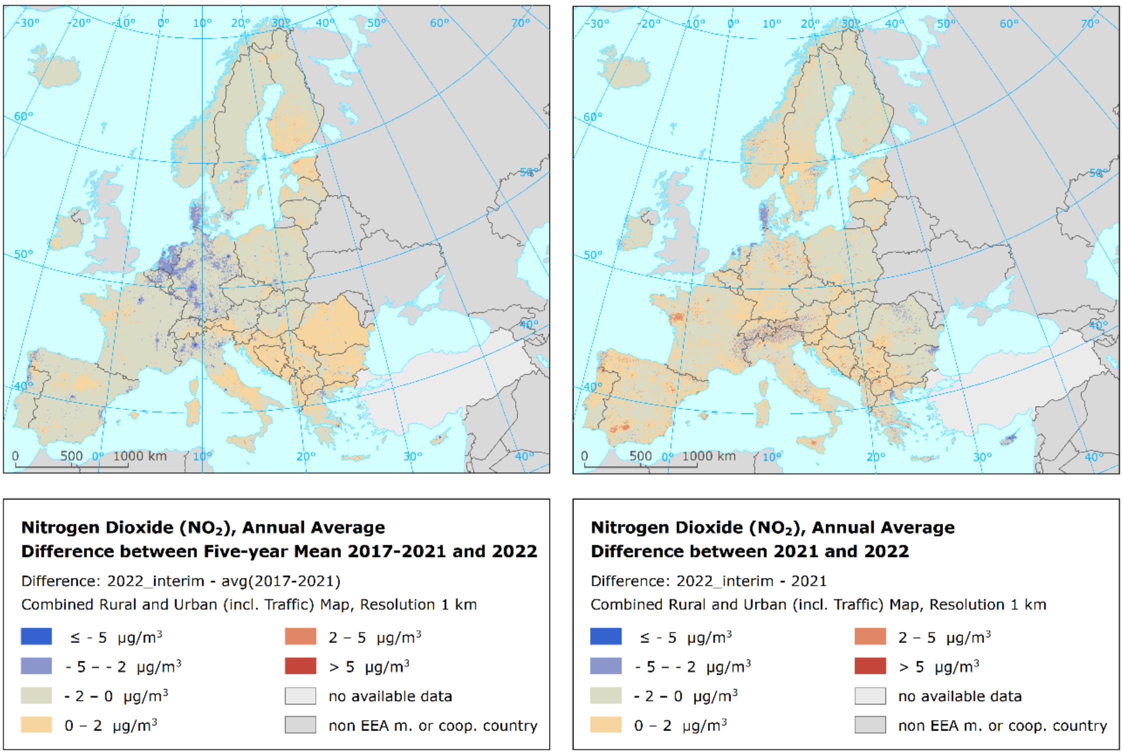

Based on the mapping results and the population density data, the population exposure estimate has been calculated. Table 6.1 gives the population frequency distribution for a limited number of exposure classes and the population-weighted concentrations for large European regions, for EU-27 and for the total mapping area. The exposure estimates for individual countries are not presented, due to their high uncertainty. As presented in Horálek et al. (2023a), the exposure estimates based on interim maps give good results for the total area and the EU-27, but somewhat poorer results for individual countries.

Table 6.1: Population exposure and population-weighted concentration, NO_2 annual average, 2022, based on interim map

Area	Population [inhbs·1000]	NO_2 – annual average, exposed population, 2022 [%]						NO_2 ann. avg.
		< 10 µg/m³	10-20 µg/m³	20-30 µg/m³	30-40 µg/m³	40-45 µg/m³	> 45 µg/m³	Pop. weighted [µg/m³·inhbs⁻¹]
Northern Europe	33 656	76.1	23.2	0.8				7.3
Western Europe (without UK)	85 680	31.5	53.6	12.7	1.7	0.5	0.0	13.5
Central Europe	166 396	23.2	66.8	9.2	0.8			13.7
Southern Europe	141 374	24.0	50.4	21.4	3.9	0.2	0.1	15.6
South-eastern Europe	46 834	17.4	60.9	20.3	1.4	0.1		15.9
Total	**473 939**	**27.9**	**55.9**	**14.1**	**1.9**	**0.2**	**0.0**	**14.0**
EU-27	**442 153**	**27.9**	**55.5**	**14.4**	**2.0**	**0.2**	**0.0**	**14.1**

Note: The percentage value "0.0" indicates that an exposed population exists, but it is small and estimated to be less than 0.05 %. Empty cells mean no population in exposure.

Based on the interim map, it is estimated that approximately 0.2 % of both the considered European and the EU-27 population has been exposed to concentrations above the EU annual limit value (ALV) of 40 µg/m³. Around 72 % of both the considered European and the EU-27 population has been exposed to concentration exceeding 10 µg/m³ (being the 2021 WHO AQG level). The population-weighted concentration of the NO_2 annual average for 2022 for both the considered European and the EU-27 population is estimated to be about 14 µg/m³.

Figure 6.1 shows, for the whole mapped area, the population frequency distribution for exposure classes with a width of 1 µg/m³. One can see the highest population frequency for classes between 8 and 16 µg/m³, continuous decline of population frequency for classes between 16 and 25 µg/m³ and continuous mild decline of population frequency for classes between 25 and 45 µg/m³.

Figure 6.1: Population frequency distribution, NO_2 annual average 2022, based on an interim map. The WHO guideline level (10 µg/m³) is marked by the green line and the annual limit value (40 µg/m³) is marked by the red line

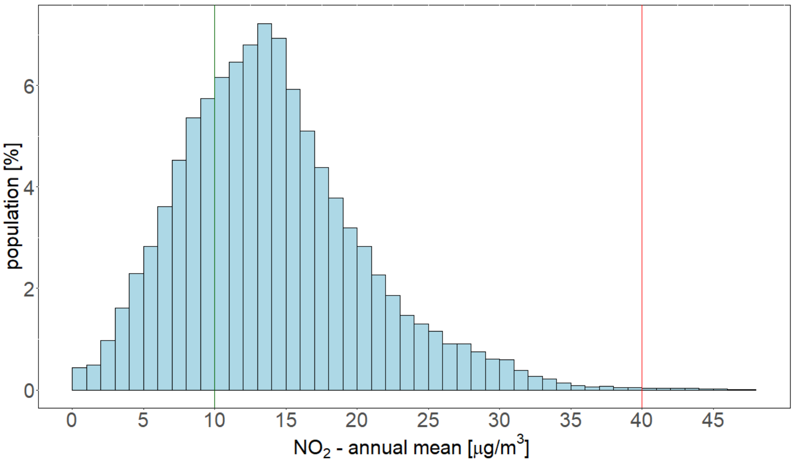

For changes in the population-weighted concentration of the NO_2 annual average in the period 2005-2022, see Figure 6.2. Again, the population-weighted concentration for the whole area including the United Kingdom is presented for the whole period including the 2022, for consistency reasons. The NO_2 concentration (in terms of annual average) shows a decrease of about 0.6 µg/m³ per year. One can see that the interim results for 2022 are well below the level of the values 2018 and 2019, after the extraordinary low concentration of 2020 due to the lockdown measures connected with the SARS-CoV-2 pandemic (in case of NO_2 especially in major cities).

Figure 6.2: Population-weighted concentration of NO_2 annual average in 2005-2022, with 2022 interim results

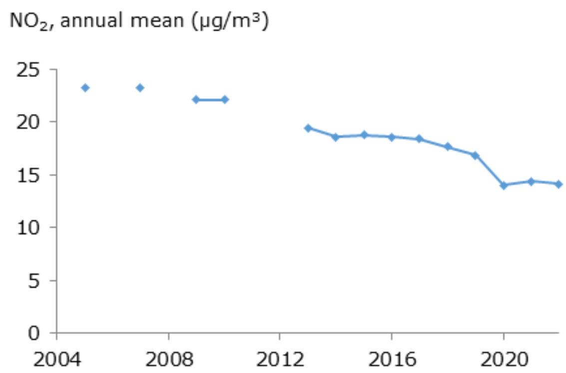

7 Production and evaluation of $PM_{2.5}$ interim mapping

The interim map creation based on the non-validated up-to-date (UTD) measurement data (as available in the E2a data set of the AQ e-reporting database), the CAMS Ensemble Forecast modelling results and other supplementary data was evaluated and recommended for regular production for PM_{10}, NO_2 and ozone, see Horálek et al. (2021a, 2021b). At that time the possibility of interim map creation for $PM_{2.5}$ was briefly checked based on 2017 data, however a low number of $PM_{2.5}$ stations with the E2a data prevented such mapping, see Horálek et al. (2021b). However, since then the number of the $PM_{2.5}$ stations with E2a data increased considerably. In addition, the need of the $PM_{2.5}$ interim map emerged for its possible use in an update of the EEA´s AQ city viewer (EEA, 2023b).

This chapter presents the evaluation of the $PM_{2.5}$ interim mapping. The evaluation is performed for the year 2021, for which the validated E1a data are already available for the purpose of the validation. Next to this, we also present the interim $PM_{2.5}$ map for 2022. The evaluation of this map using the validated E1a 2021 data has not been performed, as these data are not available yet in the time designated for this report. For the interim 2022 map, we have performed only the cross-validation based on the E2a data.

Section 7.1 evaluates the $PM_{2.5}$ interim mapping based on 2021 data, while Section 7.2 presents the $PM_{2.5}$ interim map for 2022.

7.1 Evaluation of $PM_{2.5}$ interim mapping for 2021

As a first step, the pseudo stations data have been estimated by two different approaches, as described in Section A2.1. At first, the estimates have been calculated based on the $PM_{2.5}$ E1a measurement data for 2020, the CAMS Ensemble Forecast modelling data for 2020 and 2021, and the regression relation with the $PM_{2.5}$ E2a measurement data for 2021 (see Eq. 2.4). Second, the pseudo data have been estimated based on the PM_{10} E2a measurement data for 2021, different supplementary data, and the regression relation with the $PM_{2.5}$ E2a measurement data for 2021 (see Eq. 2.5). Table 7.1 presents the regression coefficients determined for pseudo stations data estimation. The estimates based on the $PM_{2.5}$ E1a data for 2020 have been calculated using 665 rural and urban/suburban background and 293 urban/suburban traffic stations that have both E1a 2020 and E2a 2021 data available, while the estimates based on the PM_{10} E2a data for 2021 using 682 rural and urban/suburban background and 303 urban/suburban traffic stations that have both PM_{10} and $PM_{2.5}$ E2a 2021 data available.

Table 7.1: Parameters and statistics of the linear regression model for the generation of pseudo $PM_{2.5}$ data in rural and urban background and urban traffic areas for $PM_{2.5}$ annual average 2021, using $PM_{2.5}$ E1a data for 2020 (top) and PM_{10} E2a data for 2021 (bottom)

$PM_{2.5}$ - Annual average		Rural and urban background areas	Urban traffic areas
Linear regression model (LRM, Eq. 2.4)	c (constant)	1.6	1.1
	a1 ($PM_{2.5}$ annual mean 2020, E1a measurement data)	0.185	0.412
	a2 ($PM_{2.5}$ annual mean 2020 * CAMS ratio 2021/2020)	0.605	0.456
	Adjusted R^2	**0.90**	**0.92**
	Standard Error [μg/m^3]	**1.4**	**1.4**
Linear regresion model (LRM, Eq. 2.5)	c (constant)	21.4	43.2
	b (PM_{10} annual mean 2021, E2a measurement data)	0.619	0.462
	a1 (surface solar radiation 2021)	-0.003	-0.004
	a2 (latitude)	-0.224	-0.563
	a3 (longitude)	0.111	0.131
	Adjusted R^2	**0.79**	**0.71**
	Standard Error [μg.m^{-3}]	**2.2**	**2.6**

As can be seen, the estimates based on the $PM_{2.5}$ data for 2020 show stronger correlation with the $PM_{2.5}$ data for 2021, compared to the estimates based on the PM_{10} data for 2021. Based on this, we have decided to apply primarily the pseudo data estimates based on the $PM_{2.5}$ data for 2020. Thus, the pseudo data estimates based on the PM_{10} data for 2021 have been further applied only for places with no pseudo data estimates based on the $PM_{2.5}$ data for 2020.

As a next step, the pseudo data estimates have been validated based on the validated E1a $PM_{2.5}$ data for 2021, where available. Table 7.2 shows the validation of the pseudo stations, based on the E1a measurements, separately for the two types of the pseudo data.

Lower RMSE and RRMSE and higher R^2 generally indicate better performance; bias closer to zero is also an indication of better performance. Furthermore, the slope should be as close to *1* as possible and the intercept as close to *0* as possible.

Table 7.2: Validation of pseudo $PM_{2.5}$ data showing RMSE, RRMSE, bias, R^2 and linear regression from validation scatter plots for rural background (top), urban/suburban background (middle) and urban/suburban traffic stations (bottom), $PM_{2.5}$ annual mean 2021. Validation by 2021 E1a data. Units: µg.m^{-3} except RRMSE and R^2

$PM_{2.5}$ – Rural background stations							
Validation set	**Type of pseudo stations**	**N**	**RMSE**	**RRMSE**	**Bias**	**R^2**	**Regr. eq.**
E1a stations (not in E2a data set)	Based on $PM_{2.5}$ data for 2020	73	1.9	19.6%	0.2	0.871	y = 1.017x + 0.05
	Based on PM_{10} data for 2021	6	1.5	19.5%	1.4	0.904	y = 0.717x + 3.57
$PM_{2.5}$ - Urban/suburban background stations							
Validation set	**Type of pseudo stations**	**N**	**RMSE**	**RRMSE**	**Bias**	**R^2**	**Regr. eq.**
E1a stations (not in E2a data set)	Based on $PM_{2.5}$ data for 2020	197	1.3	9.6%	0.0	0.929	y = 0.927x + 1.03
	Based on PM_{10} data for 2021	41	2.4	22.1%	0.1	0.817	y = 0.797x + 2.24
$PM_{2.5}$ – Urban/suburban traffic stations							
Validation set	**Type of pseudo stations**	**N**	**RMSE**	**RRMSE**	**Bias**	**R^2**	**Regr. eq.**
E1a stations (not in E2a data set)	Based on $PM_{2.5}$ data for 2020	66	1.2	9.5%	0.3	0.903	y = 0.915x + 1.36
	Based on PM_{10} data for 2021	18	2.7	24.8%	0.6	0.921	y = 0.680x + 4.02

Looking at the results, one can see quite satisfactory results for the pseudo data based on the $PM_{2.5}$ measurements for 2020, namely in the urban background and urban traffic areas. Somewhat poorer results of the pseudo data estimates based on the PM_{10} data for 2021 are influenced by the lower number of the stations available for the validations; note that the pseudo data estimates based on PM_{10} data for 2021 are used only in the points of stations without the pseudo data based on the $PM_{2.5}$ 2020 data.

Based on the validation results, we have further used two variants of the pseudo $PM_{2.5}$ data sets, i.e. (i) pseudo data based on $PM_{2.5}$ measurements for 2020 only and (ii) pseudo data based on the $PM_{2.5}$ measurements for 2020 supplemented by the pseudo data based on the PM_{10} measurements for 2021.

Based on the E2a data and pseudo data sets in two variants (i) and (ii), CAMS Ensemble Forecast modelling data and other supplementary data as used in the regular mapping, the interim $PM_{2.5}$ annual average maps for 2021 have been created (in two variants).

Table 7.3 presents the estimated parameters of the linear regression models (*c, a_1, a_2,…*) and of the residual kriging (*nugget, sill, range*) and includes the statistical indicators of both the regression and the kriging of its residuals.

Table 7.3: Parameters and statistics of the linear regression model and ordinary kriging in rural, urban background and urban traffic areas for the interim map of $PM_{2.5}$ annual average 2021

$PM_{2.5}$ – Annual average		Variant (i) Rural areas	Variant (i) Urban b. areas	Variant (i) Urban tr. areas	Variant (ii) Rural areas	Variant (ii) Urban b. areas	Variant (ii) Urban tr. areas
Linear regresion model (LRM, Eq. 2.1)	c (constant)	0.66	0.73	0.69	0.83	0.81	0.77
	a1 (log. CAMS-ENS-FC model)	0.813	0.76	0.778	0.736	0.72	0.738
	a2 (altitude GMTED)	-0.00029			-0.00030		
	a3 (wind speed)	-0.044			-0.046		
	a4 (land cover NAT1)	*n.sign.*			*n.sign.*		
	Adjusted R^2	**0.70**	**0.45**	**0.66**	**0.60**	**0.43**	**0.62**
	Standard Error [μg/m^3]	**0.23**	**0.28**	**0.22**	**0.26**	**0.28**	**0.24**
Ordinary kriging (OK) of LRM	nugget	0.020	0.017	0.015	0.017	0.010	0.018
	sill	0.050	0.060	0.035	0.063	0.056	0.036
	range [km]	660	450	160	630	410	340
LRM + OK of its residuals	**RMSE [μg/m^3]**	**1.6**	**3.5**	**2.5**	**1.6**	**3.4**	**2.5**
	Relative RMSE [%]	**18.0%**	**28.1%**	**21.6%**	**18.7%**	**27.3%**	**21.4%**
	Bias (MPE) [μg/m^3]	**0.0**	**-0.1**	**-0.1**	**0.1**	**-0.2**	**0.0**

Table 7.4 presents the validation of the interim maps in both variants, based on the E1a station data. The validation has been performed separately for station points with and without E2a data both for separate map layers (either rural, urban background or urban traffic) and final merged map, for different area types.

Table 7.4: Validation of the interim spatial mapping results showing RMSE, RRMSE, bias, R^2 and linear regression from validation scatter plots in rural background (top), urban background (middle) and urban traffic (bottom) areas for $PM_{2.5}$ annual average 2021. Cross-validation and simple validation by E1a stations. Units: μg/m^3 except RRMSE and R^2

$PM_{2.5}$ – Annual average		N	Variant (i) RMSE	Variant (i) RRMSE	Variant (i) Bias	Variant (i) R^2	Variant (i) Lin. r. equation	Variant (ii) RMSE	Variant (ii) RRMSE	Variant (ii) Bias	Variant (ii) R^2	Variant (ii) Lin. r. equation
Rural background areas												
E2a station points, cross-val. pred.	Rural map layer	151	1.5	17.7%	0.3	0.823	y = 0.827x + 1.77	1.6	19.7%	0.3	0.779	y = 0.790x + 2.09
E2a station points, grid prediction	Rural map layer	151	1.3	15.0%	0.0	0.870	y = 0.805x + 1.60	1.3	15.4%	0.0	0.864	y = 0.789x + 1.79
	Final map		1.3	15.8%	0.1	0.854	y = 0.808x + 1.68	1.4	16.3%	0.1	0.846	y = 0.788x + 1.90
Points with no E2a station data, grid prediction	Rural map layer	93	1.8	19.0%	0.0	0.848	y = 0.797x + 1.90	1.8	18.4%	-0.1	0.860	y = 0.795x + 1.88
	Final map		1.8	18.4%	0.1	0.854	y = 0.808x + 1.68	1.6	17.2%	0.2	0.846	y = 0.788x + 1.90
Urban background areas												
E2a station points, cross-val. pred.	Urban b. map l.	585	2.5	21.2%	0.2	0.706	y = 0.762x + 3.02	2.4	20.1%	0.1	0.728	y = 0.743x + 3.17
E2a station points, grid prediction	Urban b. map l.	585	1.9	15.9%	0.1	0.832	y = 0.815x + 2.31	1.7	14.0%	0.1	0.873	y = 0.818x + 2.25
	Final map		2.1	17.4%	0.0	0.796	y = 0.791x + 2.47	2.0	16.4%	-0.1	0.805	y = 0.765x + 3.23
Points with no E2a station data, grid prediction	Urban b. map l.	298	2.9	21.4%	0.0	0.736	y = 0.765x + 3.18	2.5	18.5%	0.0	0.822	y = 0.787x + 2.49
	Final map		3.0	21.6%	0.0	0.732	y = 0.766x + 3.22	2.6	18.9%	0.0	0.796	y = 0.761x + 3.29
Urban traffic areas												
E2a station points, cross-val. pred.	Urb. traf. map l.	324	2.2	19.6%	0.1	0.799	y = 0.810x + 2.28	2.3	20.0%	0.1	0.790	y = 0.768x + 2.78
E2a station points, grid prediction	Urb. traf. map l.	324	1.8	16.0%	0.4	0.871	y = 0.875x + 1.78	1.9	17.0%	0.3	0.853	y = 0.819x + 2.36
	Final map		2.1	18.7%	-0.4	0.822	y = 0.833x + 1.53	2.1	18.8%	-0.4	0.824	y = 0.786x + 2.02
Points with no E2a station data, grid prediction	Urb. traf. map l.	107	3.8	32.7%	0.6	0.640	y = 0.722x + 3.59	3.6	31.0%	0.5	0.696	y = 0.697x + 3.83
	Final map		4.1	34.8%	-0.5	0.560	y = 0.609x + 3.81	3.9	33.6%	-0.4	0.582	y = 0.582x + 4.24

Looking at the statistics, one can state that the results are quite satisfactory in general. The mapping variant (ii) using both types of pseudo data gives slightly better results for the urban background areas, compared to the variant (i) using only the pseudo data based on $PM_{2.5}$ data for 2020. For both rural and urban traffic areas, the variant (i) shows slightly better results for areas covered by E2a stations, while the variant (ii) gives slightly better results for areas not covered by the E2a stations.

Based on the results of the analysis, we further use the mapping variant (ii) using both types of pseudo data. For future, it is recommended to use the pseudo stations based on the PM_{10} data for the actual year only in areas with poor coverage by the E2a data.

Map 7.1 presents the final merged interim map of the $PM_{2.5}$ annual average for 2021, as created by the mapping variant (ii).

Map 7.1: Interim concentration map of $PM_{2.5}$ annual average, 2021, mapping methodology using pseudo data estimated based on both $PM_{2.5}$ 2020 and PM_{10} 2021 measurements

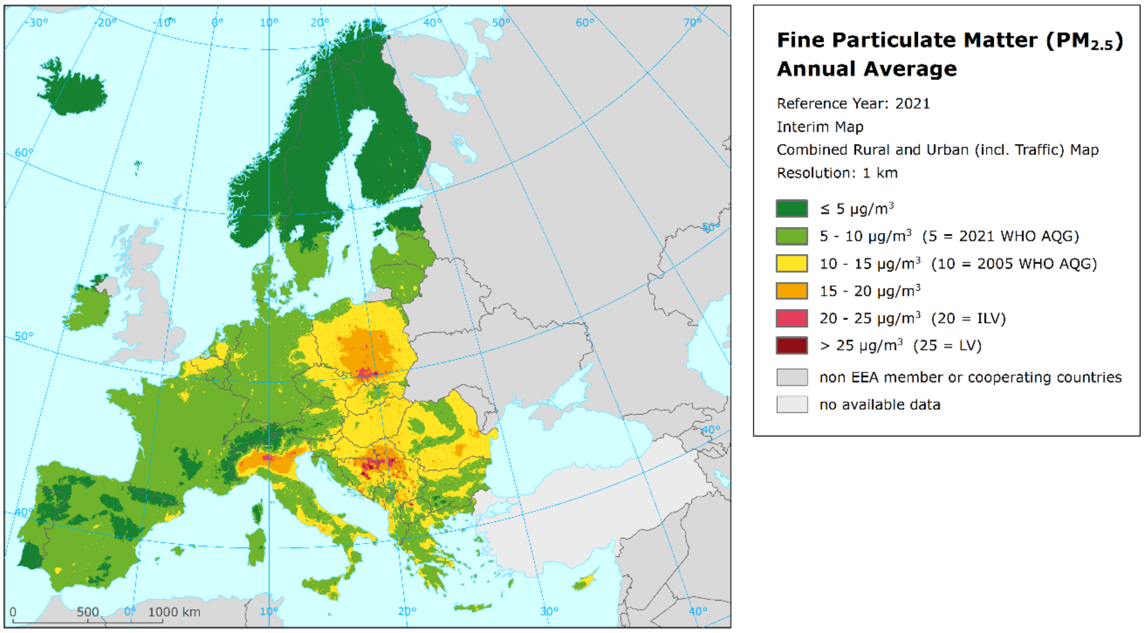

It can be concluded that the uncertainty of the map (see the relative uncertainty expressed as RRMSE, Table 7.4) is low enough to enable the interim map construction (e.g., it fulfils the data quality objectives for models as set in the AQ Directive, EC, 2008). Thus, it is recommended to include $PM_{2.5}$ in the set of air quality indicators for interim mapping. However, we also recommend to validate the $PM_{2.5}$ interim mapping for another year.

7.2 Interim $PM_{2.5}$ map for 2022

In this section, we present the interim map for 2022, created primarily based on the E2a measurement data for 2022, using the methodology evaluated for 2021 in Section 7.1.

Like for 2021, the pseudo stations data of two types have been estimated at first, i.e. based on the $PM_{2.5}$ E1a measurement data for 2021, the CAMS Ensemble Forecast modelling data for 2021 and 2022, and the regression relation with the $PM_{2.5}$ E2a measurement data for 2022 (see Eq. 2.4) and based on the PM_{10} E2a measurement data for 2022, different supplementary data, and the regression relation with the $PM_{2.5}$ E2a measurement data for 2022 (see Eq. 2.5). Table 7.5 presents the regression coefficients determined for these pseudo stations data estimations. The estimates based on the $PM_{2.5}$ E1a data for 2021 have been calculated using 813 rural and urban/suburban background and 348 urban/suburban traffic stations that have both E1a 2021 and E2a 2022 data available, while the estimates based on the PM_{10} E2a data for 2022 using 805 rural and urban/suburban background and 349 urban/suburban traffic stations that have both PM_{10} and $PM_{2.5}$ E2a 2022 data available.

Table 7.5: Parameters and statistics of the linear regression model for the generation of pseudo $PM_{2.5}$ data in rural and urban background and urban traffic areas for $PM_{2.5}$ annual average 2022, using $PM_{2.5}$ E1a data for 2021 (top) and PM_{10} E2a data for 2022 (bottom)

$PM_{2.5}$ - Annual average		Rural and urban background areas	Urban traffic areas
Linear regression model (LRM, Eq. 2.4)	c (constant)	1.5	1.2
	a1 ($PM_{2.5}$ annual mean 2021, E1a measurement data)	*n. sign.*	*n. sign.*
	a2 ($PM_{2.5}$ annual mean 2021 * CAMS ratio 2022/2021)	0.809	0.837
	Adjusted R^2	**0.90**	**0.91**
	Standard Error [µg/m^3]	**1.3**	**1.1**
Linear regresion model (LRM, Eq. 2.5)	c (constant)	31.5	62.1
	b (PM_{10} annual mean 2022, E2a measurement data)	0.625	0.432
	a1 (surface solar radiation 2022)	-0.004	-0.006
	a2 (latitude)	-0.375	-0.805
	a3 (longitude)	0.112	0.165
	Adjusted R^2	**0.81**	**0.72**
	Standard Error [µg.m^{-3}]	**1.9**	**2.3**

Similarly as in Section 7.1, the estimates based on the $PM_{2.5}$ data for 2021 show stronger correlation with the $PM_{2.5}$ data for 2022, compared to the estimates based on the PM_{10} data for 2022. This confirms the decision taken in Section 7.1 to apply primarily the pseudo data estimates based on the $PM_{2.5}$ data for Y-1. Leading from this, the pseudo data estimates based on the PM_{10} data for 2022 have been further applied only in places with no pseudo data estimates based on the $PM_{2.5}$ data for 2021. For the number of $PM_{2.5}$ data and pseudo $PM_{2.5}$ data of both types applied in the interim map creation, see Table 2.4.

Based on the E2a data and pseudo data, CAMS Ensemble Forecast modelling data and other supplementary data as used in the regular mapping, the interim $PM_{2.5}$ annual average map for 2022 has been created. Table 7.6 presents the estimated parameters of the linear regression models (*c, a_1, a_2,…*) and of the residual kriging (*nugget, sill, range*) and includes the statistical indicators of both the regression and the kriging of its residuals.

Table 7.6: Parameters and statistics of the linear regression model and ordinary kriging in rural, urban background and urban traffic areas for the interim map of $PM_{2.5}$ annual average 2022

$PM_{2.5}$ – Annual average		Variant (ii)		
		Rural areas	Urban b. areas	Urban tr. areas
Linear regresion model (LRM, Eq. 2.1)	c (constant)	0.89	0.84	0.78
	a1 (log. CAMS-ENS-FC model)	0.696	0.69	0.714
	a2 (altitude GMTED)	-0.00024		
	a3 (wind speed)	-0.053		
	a4 (land cover NAT1)	*-0.0009*		
	Adjusted R^2	**0.66**	**0.44**	**0.63**
	Standard Error [µg/m^3]	**0.22**	**0.26**	**0.23**
Ordinary kriging (OK) of LRM	nugget	0.022	0.017	0.012
	sill	0.045	0.049	0.035
	range [km]	640	210	330
LRM + OK of its residuals	**RMSE [µg/m^3]**	**2.0**	**2.5**	**2.2**
	Relative RMSE [%]	**23.4%**	**21.3%**	**20.4%**
	Bias (MPE) [µg/m^3]	**-0.1**	**0.0**	**0.0**

Map 7.2 presents the interim map for the $PM_{2.5}$ annual average 2022, as the result of interpolation and merging of the separate map layers as described above. Dark red areas show concentrations above

the EU annual limit value (LV) of 25 μg/m³. Red areas show concentrations above the indicative LV of 20 μg/m³ defined as Stage 2 (ILV). Dark green indicates the areas where the $PM_{2.5}$ annual average concentration is below the WHO Air Quality Guideline level of 5 μg/m³ (WHO, 2021).

Map 7.2: Interim concentration map of $PM_{2.5}$ annual average, 2022

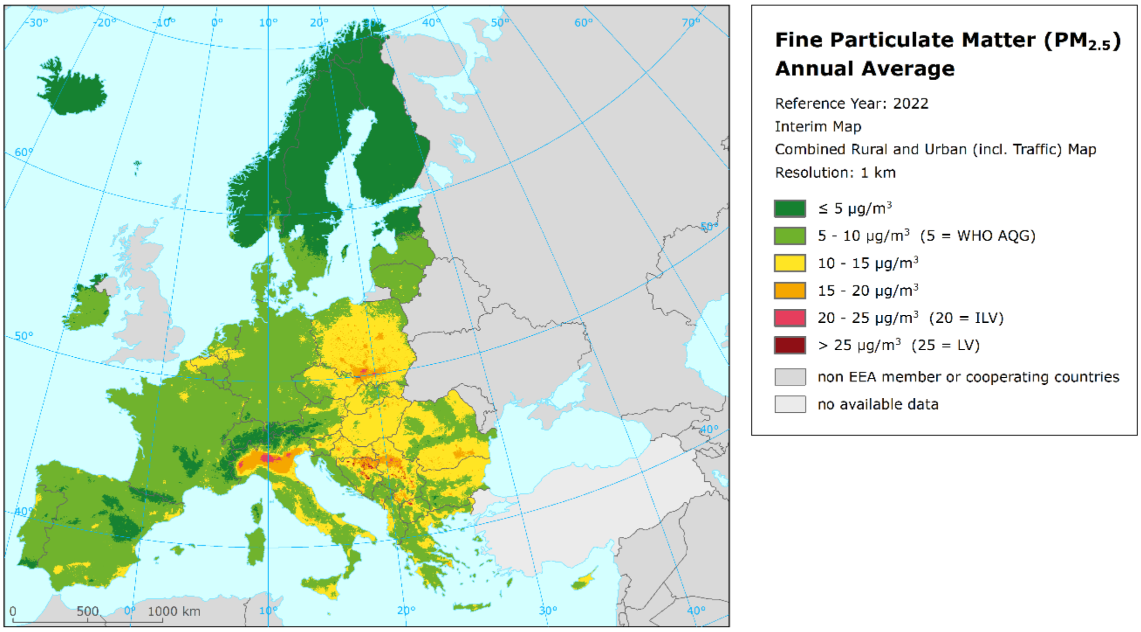

The map shows $PM_{2.5}$ concentrations above the annual LV in some scattered urban areas of Bosnia and Herzegovina, Croatia, Montenegro, North Macedonia, Serbia, and Kosovo. Concentrations above the ILV appear in the Po Valley (in northern Italy), in the Krakow – Katowice (Poland) – Ostrava (Czechia) industrial region, in large areas of central Serbia and north of Bosnia and Herzegovina and in some other areas of Balkan countries and Poland.

The relative mean uncertainty (Relative RMSE) of this map is 23 % for rural areas and 21 % for urban background areas (Table 7.6). However, these uncertainty estimates are based on the non-validated E2a data and are valid only for areas covered by the E2a stations. The complete validation of the interim $PM_{2.5}$ map can only be done when the validated E1a data for 2022 are available.

Based on the mapping results and the population density data, the population exposure estimates have been calculated. Table 7.7 gives the population frequency distribution for a limited number of exposure classes and the population-weighted concentration for large European regions, for EU-27 and for the total presented area.

Based on the interim map, it is estimated that 0.7 % of population living in the considered (i.e. presented) European area has been exposed to concentrations above the EU annual limit value (LV) of 25 μg/m³. For the EU-27, almost no population (i.e. less than 0.05%) is estimated to be exposed to LV exceedances. About 97 % of the population living in both the considered European area and the EU-27 has been exposed to concentrations above the WHO Air Quality Guideline level of 5 μg/m³. The population-weighted concentration of the $PM_{2.5}$ annual average for 2022 is estimated to be 11.5 μg/m³ for the EEA member and cooperating countries and 11.3 μg/m³ for the EU-27.

Table 7.7: Population exposure and population-weighted concentration, $PM_{2.5}$ annual average, 2022, based on the interim map

Area	Population [inhbs·1000]	$PM_{2.5}$ – annual average, exposed population, 2022 [%]						$PM_{2.5}$ ann. avg.
		< 5 µg/m³	5-10 µg/m³	10-15 µg/m³	15-20 µg/m³	20-25 µg/m³	> 25 µg/m³	Pop. weighted [µg/m³·inhbs⁻¹]
Northern Europe	33 656	36.1	56.5	7.4				6.2
Western Europe (without UK)	85 680	0.3	59.6	40.2				9.5
Central Europe	166 396	0.1	45.8	35.9	16.0	2.1		11.6
Southern Europe	141 374	0.2	30.6	49.9	16.0	3.3		12.1
South-eastern Europe	46 834	0.0	7.1	43.4	33.6	9.6	6.3	15.9
Total	**473 939**	**2.6**	**40.2**	**39.7**	**14.0**	**2.8**	**0.7**	**11.5**
EU-27	**442 153**	**2.3**	**39.4**	**42.7**	**13.6**	**1.9**	**0.0**	**11.3**

Note: Empty cells mean no population in exposure.

Figure 7.1 shows, for the whole mapped area, the population frequency distribution for exposure classes with a width of 0.5 µg/m³. The highest population frequency is found for classes between 8 and 12 µg/m³. A quite continuous decline of population frequency can be seen for population classes beyond 14 µg/m³.

Figure 7.1: Population frequency distribution, $PM_{2.5}$ annual average, 2022. The WHO AQG level (5 µg/m³) is marked by the green line, the old 2005 WHO AQG level (10 µg/m³) is marked by the yellow line, the EU annual indicative limit value (20 µg/m³) is marked by the orange line and the EU annual limit value (25 µg/m³) is marked by the red line

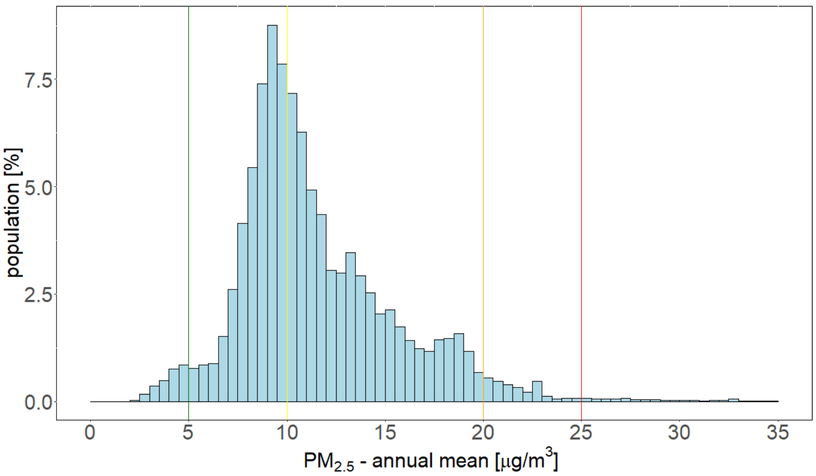

Note: Apart from the population distribution shown in graph, it was estimated that 0.02 % of population lived in areas with $PM_{2.5}$ annual average concentration in between 35 and 42 µg/m³.

8 Conclusions

The report presents the interim 2022 maps for PM_{10} annual average, NO_2 annual average and the ozone indicator SOMO35. The maps have been produced based on the non-validated E2a (UTD) data of the AQ e-reporting database, the CAMS Ensemble Forecast modelling data and other supplementary data. Together with the concentration maps, the difference maps between five-year mean 2017-2021 and 2021 and between the years 2021 and 2022 are presented (using the 2017-2021 regular and the 2022 interim maps), as well as basic exposure estimates based on the interim maps.

For PM_{10}, concentrations above the annual LV were estimated only in urban areas around Balkan cities (Bosnia and Herzegovina, Northern Macedonia and Serbia). In addition to that, there are areas in the Po Valley (in Italy) and smaller disconnected areas in Poland, Spain and Balkan countries where PM_{10} concentrations of 30-40 µg/m^3 have been estimated.

In the case of O_3, southern Europe shows higher ozone SOMO35 concentrations than northern Europe. Higher levels of ozone also occur more frequently in mountainous areas south of 50 degrees latitude than in lowlands. In 2022, SOMO35 levels > 6 000 µg/m^3·d were estimated in almost all of Italy, in much of the Balkan countries, in a large area of Spain and France, in central Europe (parts of Germany, Austria, Hungary, Switzerland) and even in small parts of northern Europe in Iceland and Norway.

In the case of NO_2, the areas with the highest concentrations, but in 2022 below the annual limit value of 40 µg/m^3 for NO_2, include urbanized parts of some large cities, particularly Paris, Rome, Naples, Milan, Madrid, Barcelona and Athens. Areas above 20 µg/m^3 can be found in the Po Valley, the Benelux, the German Ruhr region, in the Île de France region, around Rome and Naples and in the Krakow – Katowice (PL) – Ostrava (CZ) industrial region. Some other cities show NO_2 levels above 20 µg/m^3. Most of the European area shows NO_2 levels below 20 µg/m^3 or even below 10 µg/m^3.

Uncertainty estimates based on the cross-validation of the E2a data have been performed for all interim maps, showing quite satisfactory results in general. However, these uncertainty estimates are based on the non-validated E2a data and are valid for areas covered by the E2a measurements only. The complete validation of the interim maps should be done when the validated E1a data for 2022 are available.

In the report, population exposure for only large European regions, EU27 and the total mapped area has been presented. The more detailed exposure estimates for particular European countries will be presented in 2024, in the ETC HE regular mapping report on the 2022 air quality maps created based on the validated data E1a.

Next to the creation of the regular interim maps for PM_{10}, O_3 and NO_2, interim mapping of $PM_{2.5}$ has been tested and evaluated. The $PM_{2.5}$ interim map for 2021 has been verified based on the validated E1a measurement data. Based on the analysis performed, the conclusion is that the uncertainty of this map is low enough to enable the interim map construction. Thus, it is recommended to include $PM_{2.5}$ in the set of air quality indicators for interim mapping.

Based on the methodology evaluated for 2021, the $PM_{2.5}$ interim map for 2022 has been also constructed. The highest $PM_{2.5}$ concentrations appear to be in some scattered urban areas of Bosnia and Herzegovina, Croatia, Montenegro, North Macedonia, and Serbia.

List of abbreviations

Abbreviation	Name	Reference
ALV	Annual Limit Value	
AQ	Air Quality	
AQG	Air Quality Guideline of the WHO	
CLC	CORINE Land Cover	https://land.copernicus.eu/pan-european/corine-land-cover
CORINE	Co-ORdinated INformation on the Environment	https://land.copernicus.eu/pan-european/corine-land-cover
CTM	Chemical Transport model	
ECMWF	European Centre for Medium-Range Weather Forecasts	https://www.ecmwf.int/
EBAS	EMEP dataBASe	https://ebas.nilu.no/
EEA	European Environment Agency	www.eea.europa.eu
EMEP	European Monitoring and Evaluation Programme	https://www.emep.int/
ETC HE	European Topic Centre on Human health and the Environment	https://www.eionet.europa.eu/etcs
EU	European Union	https://european-union.europa.eu
GMTED	Global multi-resolution terrain elevation data	
GRIP	Global Roads Inventory Dataset	
ILV	Indicative Limit Value	
JRC	Joint Research Centre	https://ec.europa.eu/info/departments/joint-research-centre_en
LV	Limit Value	http://eur-lex.europa.eu/LexUriServ/LexUriServ.do?uri=OJ:L:2008:152:0001:0044:EN:PDF
NILU	Norwegian Institute for Air Research	https://www.nilu.no/
NO_2	Nitrogen dioxide	
O_3	Ozone	
ORNL	Oak Ridge National Laboratory	https://www.ornl.gov/
PM_{10}	Particulate Matter with a diameter of 10 micrometres or less	
$PM_{2.5}$	Particulate Matter with a diameter of 2.5 micrometres or less	
R^2	Coefficient of determination	
RIMM	Regression – Interpolation – Merging Mapping	
RMSE	Root Mean Square Error	
SOMO35	Sum of Ozone Maximum daily 8-hour means Over 35 ppb (i.e. 70 µg/m^3)	
UTC	Coordinated Universal Time	
WHO	World Health Organization	https://www.who.int/

References

Cressie, N., 1993, *Statistics for spatial data,* Wiley series, New York.

Danielson, J. J. and Gesch, D. B., 2011, *Global multi-resolution terrain elevation data 2010 (GMTED2010)*, U.S. Geological Survey Open-File Report, pp. 2011-1073 (https://pubs.er.usgs.gov/publication/ofr20111073) accessed 19 November 2020.

Defra, 2023, *UK Air information resource, Data archive*, UK Department for Environment Food & Rural Affairs (https://uk-air.defra.gov.uk/data/). Data extracted in April 2023.

EC, 2008, Directive 2008/50/EC of the European Parliament and of the Council of 21 May 2008 on ambient air quality and cleaner air for Europe, OJ L 152, 11.06.2008, 1-44 (http://eur-lex.europa.eu/LexUriServ/LexUriServ.do?uri=OJ:L:2008:152:0001:0044:EN:PDF) accessed 26 May 2021.

ECMWF, 2023, CAMS Regional: European air quality analysis and forecast data documentation. WWW: (https://confluence.ecmwf.int/display/CKB/CAMS+Regional%3A+European+air+quality+analysis+and+forecast+data+documentation) accessed 2 October 2023.

EEA, 2022, *Air Quality e-Reporting. Air quality database* (https://www.eea.europa.eu/data-and-maps/data/aqereporting-8). Data extracted in March 2022.

EEA, 2023a, *Air Quality e-Reporting. Air quality database* (https://www.eea.europa.eu/data-and-maps/data/aqereporting-8). Data extracted in March 2023.

EEA, 2023b, *European city air quality viewer* (https://www.eea.europa.eu/themes/air/urban-air-quality/european-city-air-quality-viewer) accessed 12 October 2023.

EU, 2020, *Corine land cover 2018 (CLC2018) raster data*, 100x100m^2 gridded version 2020_20 (https://land.copernicus.eu/pan-european/corine-land-cover/clc2018) accessed 19 November 2020.

Eurostat, 2014, *GEOSTAT 2011 grid dataset. Population distribution dataset* (http://ec.europa.eu/eurostat/web/gisco/geodata/reference-data/population-distribution-demography) accessed 26 August 2020.

Gilbert, R. O., 1987, *Statistical Methods for Environmental Pollution Monitoring*, Van Nostrand Reinhold, New York.

Horálek, J., et al., 2021a, *Potential use of CAMS modelling results in air quality mapping under ETC/ATNI*, Eionet Report ETC/ATNI 2019/17 (https://doi.org/10.5281/zenodo.4627762) accessed 15 June 2021.

Horálek, J., et al., 2021b, *European air quality interim mapping under ETC/ATNI*, Eionet Report ETC/ATNI 2020/11 (https://doi.org/10.5281/zenodo.5564555) accessed 12 October 2021.

Horálek, J., et al., 2023a, *Interim European air quality maps for 2021*, Eionet Report – ETC HE 2022/4 (https://doi.org/10.5281/zenodo7565623) accessed 14 September 2023.

Horálek, J., et al., 2023b, *Air quality maps of EEA member and cooperating countries for 2021*, Eionet Report ETC HE 2023/3, *in preparation*.

Kuenen, J., et al., 2021, *Copernicus Atmosphere Monitoring Service regional emissions version 4.2* (CAMS-REG-v4.2) Copernicus Atmosphere Monitoring Service [publisher] ECCAD [distributor], (https://doi.org/10.24380/0vzb-a387) accessed 6 August 2022.

Meijer, J. R., et al., 2018, 'Global patterns of current and future road infrastructure', *Environmental Research Letters* 13, 0640 (https://doi.org/10.1088/1748-9326/aabd42) accessed 10 June 2019.

METEO FRANCE, et al., 2022, *CAMS European air quality forecasts, ENSEMBLE data. Copernicus Atmosphere Monitoring Service (CAMS) Atmosphere Data Store (ADS)* (https://ads.atmosphere.copernicus.eu/cdsapp#!/dataset/cams-europe-air-quality-forecasts?tab=overview) accessed on 2 October 2023.

NILU, 2023, *EBAS, database of atmospheric chemical composition and physical properties* (http://ebas.nilu.no). Data extracted in April 2023.

van Geffen, J., et al., 2020, 'S5P TROPOMI NO_2 slant column retrieval: Method, stability, uncertainties and comparisons with OMI', *Atmospheric Measurement Techniques* 13, pp. 1315–1335 (https://doi.org/10.5194/amt-13-1315-2020) accessed 30 August 2021.

Veefkind, J. P., et al., 2012. 'TROPOMI on the ESA Sentinel-5 Precursor: A GMES mission for global observations of the atmospheric composition for climate, air quality and ozone layer applications', *Remote Sensing of Environment* 120, pp. 70–83 (https://doi.org/10.1016/j.rse.2011.09.027) accessed 30 August 2021.

WHO, 2021, WHO global air quality guidelines: particulate matter ($PM_{2.5}$ and PM_{10}), ozone, nitrogen dioxide, sulfur dioxide and carbon monoxide, World Health Organization (https://apps.who.int/iris/handle/10665/345329) accessed 22 September 2022.

Annex Technical details and uncertainties of interim maps

This Annex presents different technical details on the interim maps presented in this report. Sections A.1, A.2 and A.3 gives technical details and uncertainty estimates of the 2022 interim maps for PM_{10}, ozone and NO_2, respectively. Section A.4 shows the air quality measurement stations used for the mapping and validation of the 2021 interim map for $PM_{2,5}$.

A.1 Particulate matter PM_{10}

This section presents the technical details and uncertainty estimates of the PM_{10} 2022 annual average interim map as presented in Map 4.1.

Like in Horálek et al. (2021b), at first the pseudo stations data have been estimated. The estimates have been calculated based on the E1a measurement data for 2021, the CAMS Ensemble Forecast modelling data for 2021 and 2022, and the regression relation with the E2a measurement data for 2022. Table A.1 presents the regression coefficients determined for pseudo stations data estimation, based on the 1362 rural and urban/suburban background and 613 urban/suburban traffic stations that have both E1a 2021 and E2a 2022 measurements available (see Sections 2.2 and 3.1). Next to this, it presents the statistics showing the tentative quality of the estimate.

Table A.1: Parameters and statistics of the linear regression model for the generation of pseudo PM_{10} data in rural and urban background and urban traffic areas, for PM_{10} annual average 2022

PM_{10} – Annual average		**Rural and urban background areas**	**Urban traffic areas**
Linear regression model (LRM, Eq. 2.4)	c (constant)	2.3	2.3
	a1 (PM_{10} annual mean 2021, E1a data)	*n. sign.*	*n. sign.*
	a2 (PM_{10} annual mean 2021 * CAMS ratio 2022/2021)	0.833	0.854
	Adjusted R^2	**0.89**	**0.83**
	Standard Error [µg/m³]	**1.9**	**2.6**

Based on the E2a data and pseudo data, CAMS Ensemble Forecast modelling data and other supplementary data as used in the regular mapping, the interim PM_{10} annual average map for 2022 has been created (see Map 4.1). Table A.2 presents the estimated parameters of the linear regression models (*c, a_1, a_2,…*) and of the residual kriging (*nugget, sill, range*) and includes the statistical indicators of both the regression and the kriging of its residuals.

Table A.2 shows that the uncertainty of the interim map of PM_{10} annual average expressed by RMSE is about 3 µg/m³ for both the rural the urban background areas and 4 µg/m³ for the urban traffic areas. The relative mean uncertainty (Relative RMSE) of this map is 19 % for rural areas, 17 % for urban background areas, and 20 % for urban traffic areas, respectively. However, these uncertainty estimates are based on the non-validated E2a data and are valid only for areas covered by the E2a stations. The complete validation of the interim PM_{10} map can only be done when the validated E1a data for 2022 are available.

Table A.2: Parameters and statistics of the linear regression model and ordinary kriging in rural, urban background and urban traffic areas for the interim map of PM_{10} annual average 2022

PM_{10}		Annual average		
		Rural areas	Urban b. areas	Urban tr.. areas
Linear regresion model (LRM, Eq. 2.1)	c (constant)	1.56	1.18	1.87
	a1 (log. CAMS-ENS FC model)	0.732	0.68	0.487
	a2 (altitude GMTED)	-0.00012		
	a3 (relative humidity)	n.sign.		
	a4 (wind speed)	-0.011		-0.041
	a5 (land cover NAT1)	-0.0010		
	Adjusted R^2	**0.62**	**0.39**	**0.42**
	Standard Error [μg/m^3]	**0.23**	**0.23**	**0.23**
Ordinary kriging (OK) of LRM residuals	nugget	0.018	0.014	0.021
	sill	0.054	0.042	0.044
	range [km]	640	220	610
LRM + OK of its residuals	**RMSE [μg/m^3]**	**2.8**	**3.3**	**4.2**
	Relative RMSE [%]	**19.4**	**16.9**	**20.2**
	Bias (MPE) [μg/m^3]	**0.2**	**0.0**	**-0.2**
	R^2 of cross.-val. regr. equation	**0.72**	**0.68**	**0.59**
	Slope of cross-val. regr. equation	**0.74**	**0.76**	**0.60**
	Intercept of cross-val. regr. equation	**4.0**	**4.7**	**8.3**

A.2 Ozone

Similarly as in Horálek et al. (2023a), no pseudo stations for ozone have been used, due to a quite complete spatial coverage of the E2a data. Based on the E2a data, CAMS Ensemble Forecast modelling data and other supplementary data as used in the regular mapping, the interim map of the ozone indicator SOMO35 for 2022 has been created (see Map 5.1). Table A.3 presents the estimated parameters of the linear regression models (c, a_1, a_2,…) and of the residual kriging (*nugget, sill, range*) and includes the statistical indicators of the regression and the kriging of its residuals.

Table A.3: Parameters and statistics of the linear regression model and ordinary kriging in rural and urban background areas for the interim map of ozone indicator SOMO35 for 2022

Ozone – SOMO35		Rural background areas	Urban background areas
Linear regresion model (LRM, Eq. 2.1)	c (constant)	474	2623
	a1 (CAMS-ENS-FC model)	1.02	0.83
	a2 (altitude GMTED)	3.11	
	a3 (wind speed)		-469.1
	a4 (s. solar radiation)	*n.sign.*	*n.sign.*
	Adjusted R^2	**0.62**	**0.53**
	Standard Error [μg/m^3·d]	**1401**	**1430**
Ord. krig. (OK) of LRM residuals	nugget	1.0E+06	7.0E+05
	sill	1.8E+06	1.4E+06
	range [km]	260	120
LRM + OK of its residuals	**RMSE [[μg/m^3·d]**	**1315**	**1196**
	Relative RMSE [%]	**23.0**	**24.5**
	Bias (MPE) [μg/m^3·d]	**17**	**12**
	R^2 of cross.-val. regr. equation	**0.66**	**0.67**
	Slope of cross-val. regr. equation	**0.67**	**0.69**
	Intercept of cross-val. regr. equation	**1917**	**1550**

Table A.3 shows that the uncertainty of the interim map of ozone indicator SOMO35 expressed by RMSE is 1315 μg/m^3·d for the rural areas and 1196 μg/m^3·d for the urban background areas. The relative mean uncertainty (Relative RMSE) of this map is 23 % for the rural areas and 25 % for the urban background areas. These uncertainty estimates are based on the non-validated E2a data and are valid only for areas covered by the E2a stations. The complete validation of the interim ozone map can only be done when the validated E1a data for 2022 are available.

A.3 Nitrogen dioxide

As a first step for the interim NO_2 annual average 2022 map creation, the pseudo stations data have been estimated, based on the E1a measurement data for 2021, the Sentinel-5P satellite data for 2021 and 2022, and the regression relation with the E2a measurement 2022 data. Table A.4 presents the regression coefficients determined for pseudo stations data estimation, based on the 1573 rural and urban/suburban background and 757 urban/suburban traffic stations that have both E1a 2021 and E2a 2022 measurements available (see Sections 2.2 and 3.1). Apart from this, it gives the statistics showing the tentative quality of the estimate.

Table A.4: Parameters and statistics of the linear regression model for generation of pseudo NO_2 data in rural and urban background and urban traffic areas, for NO_2 annual average 2022

NO_2 – Annual average		Rural and urban background areas	Urban traffic areas
Linear regression model (LRM, Eq. 2.4)	c (constant)	0.2	1.7
	a1 (NO_2 annual mean 2020, E1a data)	0.852	0.915
	a2 (NO_2 annual mean 2020 * Sentinel-5P ratio 2021/2020)	0.123	*n.sign.*
	Adjusted R^2	**0.94**	**0.91**
	Standard Error [μg/m^3]	**1.7**	**2.5**

Based on the E2a data and pseudo data, CAMS Ensemble Forecast modelling data, Sentinel-5P satellite data and other supplementary data as used in the regular mapping, the interim NO_2 annual average map for 2022 has been created (see Map 6.1). Table A.5 presents the estimated parameters of the linear regression models (c, a_1, a_2,…) and of the residual kriging (*nugget, sill, range*) and includes the statistical indicators of both the regression and the kriging of its residuals.

Table A.5: Parameters and statistics of the linear regression model and ordinary kriging in rural, urban background and urban traffic areas for the interim map of NO_2 annual average 2022

NO_2		Annual average		
		Rural areas	Urb. b. areas	Urb. tr. areas
Linear regresion model (LRM, Eq. 2.1)	c (constant)	5.5	13.6	20.28
	a1 (CAMS-ENS-FC model)	0.347	0.227	0.201
	a6 (satellite Sentinel-5P)	1.16	1.282	1.287
	a2 (altitude)	-0.0062		
	a3 (altitude_5km_radius)	0.0061		
	a4 (wind speed)	-0.82	-1.892	-2.172
	a7 (population*1000)	0.00035	0.00019	
	a8 (NAT_1km)		-0.0411	
	a9 (AGR_1km)		-0.0253	
	a10 (TRAF_1km)		0.0581	
	a11 (LDR_5km_radius)	*n.sign.*	*n.sign.*	0.0970
	a12 (HDR_5km_radius)		*n.sign.*	0.1666
	a13 (NAT_5km_radius)	-0.0391		
	Adjusted R^2	**0.75**	**0.49**	**0.42**
	Standard Error [μg/m³]	**2.1**	**4.3**	**6.3**
Ordinary kriging (OK) of LRM residuals	nugget	2	10	21
	sill	4	14	34
	range [km]	100	230	130
LRM + OK of its residuals	**RMSE [μg/m³]**	**1.8**	**3.6**	**5.9**
	Relative RMSE [%]	**27.5**	**23.8**	**24.2**
	Bias (MPE) [μg/m³]	**0.1**	**0.0**	**-0.1**
	R^2 of cross.-val. regr. equation	**0.82**	**0.62**	**0.53**
	Slope of cross-val. regr. equation	**0.82**	**0.63**	**0.54**
	Intercept of cross-val. regr. equation	**1.3**	**5.7**	**11.1**

Table A.5 shows that the uncertainty of the interim map of NO_2 annual average expressed by RMSE is about 2 μg/m³ for the rural areas, 4 μg/m³ for the urban background areas, and 6 μg/m³ for the urban traffic areas, respectively. The relative mean uncertainty (Relative RMSE) of this map is 28 % for rural areas and 24 % for both urban background and urban traffic areas. However, like for PM_{10} and ozone, these uncertainty estimates are based on the non-validated E2a data and are valid only for areas covered by the E2a stations. The complete validation of the interim NO_2 map can only be done when the validated E1a data for 2022 are available.

A.4 Evaluation of $PM_{2.5}$ interim mapping

This section presents the air quality measurement stations used for the mapping and validation of 2021 interim map for $PM_{2,5}$ as presented in Map 7.1. The technical details and uncertainty estimates of the $PM_{2.5}$ annual average interim maps for 2021 and 2022 are presented directly in Chapter 7.

Map A.1 shows the spatial distribution of the rural, urban/suburban background and urban/suburban traffic stations used in the interim 2021 $PM_{2.5}$ mapping (in green, blue and orange) and validation (in red). In all figures, the true stations (in green), the pseudo stations based on $PM_{2.5}$ data for 2020 (in blue) and the pseudo stations based on PM_{10} data for 2021 (in orange) are distinguished.

Map A.1: Spatial distribution of $PM_{2.5}$ stations used in mapping and validation, 2021

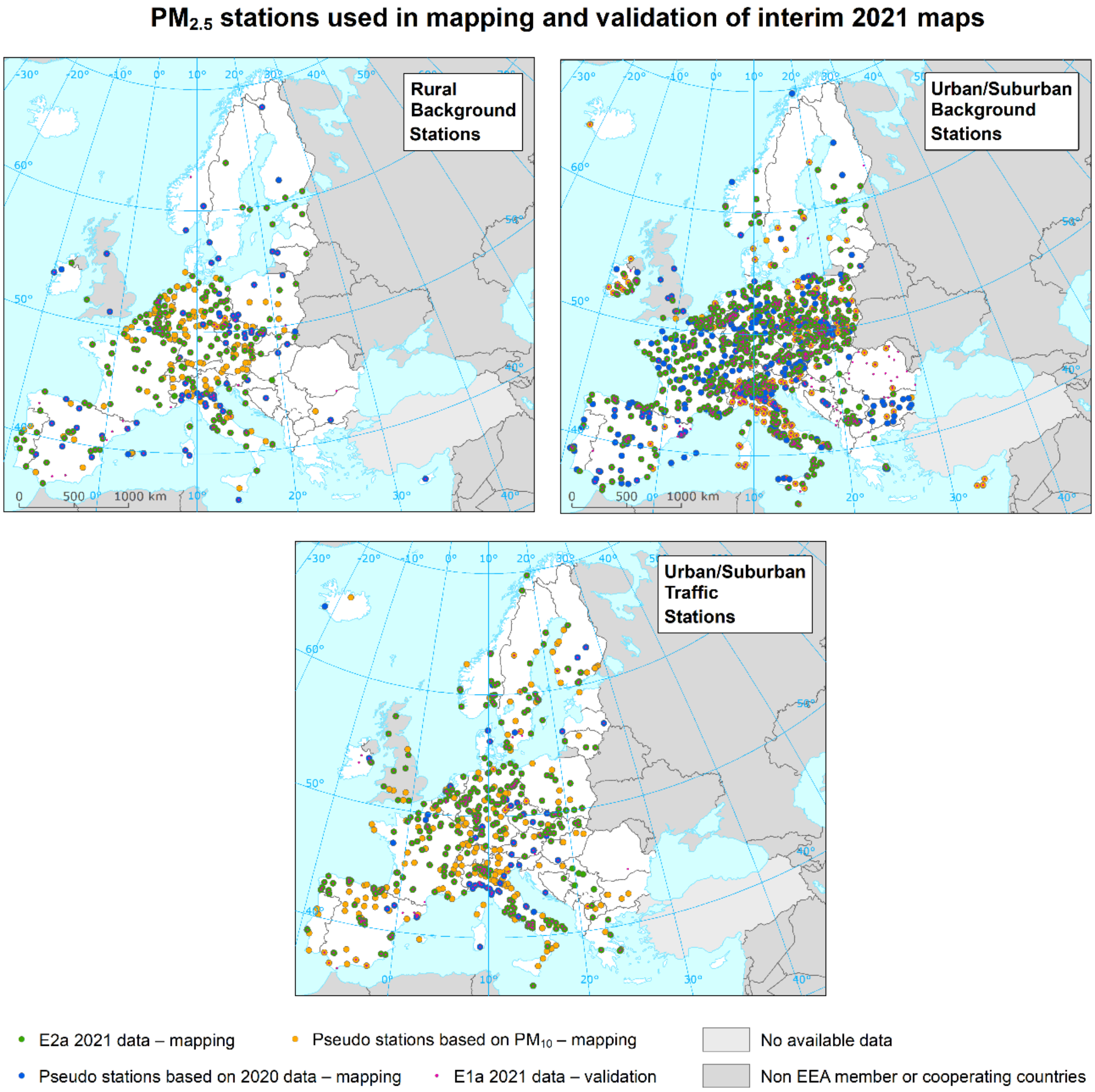

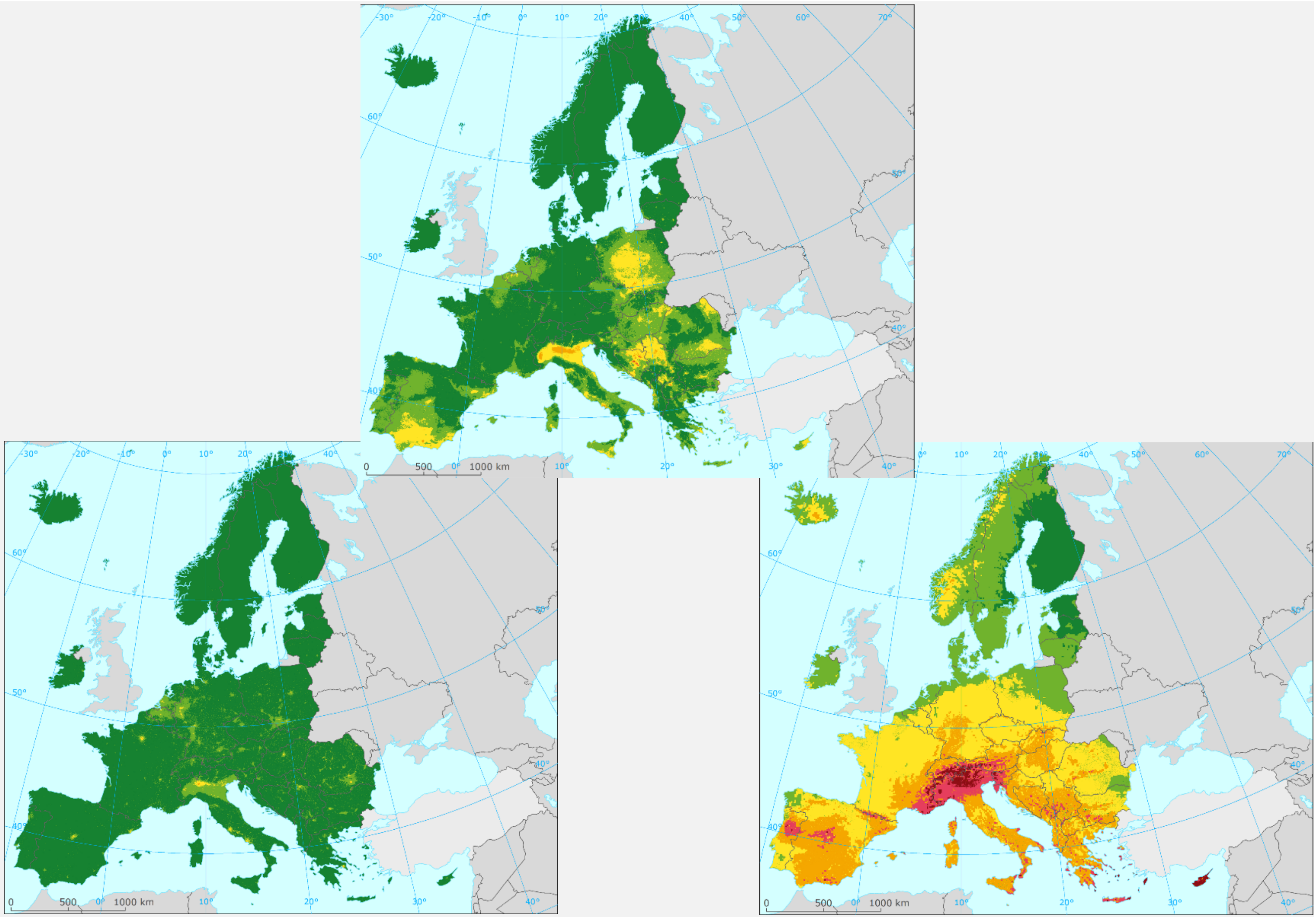

European Topic Centre on
Human Health and the Environment
https://www.eionet.europa.eu/etcs/etc-he

The European Topic Centre on Human Health and the Environment (ETC HE) is a consortium of European institutes under contract of the European Environment Agency.

European Environment Agency
European Topic Centre
Human health and the environment